

Holographic entanglement renormalisation for fermionic quantum matter: geometrical and topological aspects

Abhirup Mukherjee, Siddhartha Patra, Siddhartha Lal

Department of Physical Sciences, Indian Institute of Science Education and Research-Kolkata, W.B. 741246, India

E-mail: am18ip014@iiserkol.ac.in , sp14ip022@iiserkol.ac.in , slal@iiserkol.ac.in

ABSTRACT: On performing a sequence of renormalisation group (RG) transformations on a system of two-dimensional non-interacting Dirac fermions placed on a torus, we demonstrate the emergence of an additional spatial dimension arising out of the scaling of multipartite entanglement. The renormalisation of the entanglement under this flow exhibits a hierarchy that exists across scales as well as across number of parties. Geometric measures defined in this emergent space, such as distances and curvature, can be related to the RG beta function of the coupling g responsible for the spectral gap. This establishes a holographic connection between the spatial geometry of the emergent space in the bulk and the entanglement properties of the quantum theory lying on its boundary. Depending on the anomalous dimension of the coupling g , three classes of spaces (bounded, unbounded and flat) are generated from the RG. We show that changing from one class to another involves a topological transition. By minimising the central charge of the conformal field theory describing the noninteracting electrons under the RG flow, the RG transformations are shown to satisfy the c -theorem of Zamolodchikov. This is shown to possess a dual within the emergent geometric space, in the form of a convergence parameter that is minimised at large distances. In the presence of an Aharonov-Bohm flux, the entanglement gains a geometry-independent piece which is shown to be topological, sensitive to changes in boundary conditions, and can be related to the Luttinger volume of the system of electrons. In the presence of a strong transverse magnetic field, the system becomes insulating and Luttinger's theorem does not hold. We show instead that the entanglement contains a term that can be related to the Chern numbers of the quantum Hall states. This yields a relation between the topological invariants of the metallic and the quantum Hall systems.

Contents

1	Introduction	1
2	Preliminaries and definitions	4
2.1	The system	4
2.2	Entanglement measures	5
2.3	Luttinger volume	5
3	Entanglement hierarchy in mixed momentum and real space	6
4	Holographic geometry of the RG flow	10
4.1	EHM and the Ryu-Takayanagi bound for the gapless and gapped cases	10
4.2	RG evolution as the emergent dimension	11
4.3	Curvature of the emergent space	14
4.4	Topological nature of curvature sign	15
4.5	Embedding the emergent dimension on a metric space	18
4.6	Kinematics of the RG flows	18
4.7	Extension to the massive case	19
5	Topological content of the entanglement spectrum	20
5.1	Luttinger’s volume for massless 2D electrons	21
5.2	Chern number of the integer quantum Hall state	24
6	Conclusions and Outlook	26
A	Appendix: Reduction of the $2+1$-D system to a tower of $1+1$-D massive modes	37
B	Appendix: Evaluation of the multi-partite information	38
C	Appendix: Evaluation of the contour integral that counts poles	39

1 Introduction

Role of entanglement in fermionic systems

The present millennium has seen a rapid surge in the use of quantum entanglement towards the study of quantum and condensed matter systems [1–6]. Being non-local by nature, entanglement is helpful in tracking quantum correlations among particles across both small and large distances, offering valuable insight into the nature of the ground state and the low-energy excitations. For instance, entanglement entropy of subsystems is at the heart of understanding topological ordered states of matter [7–27]. Here, an additional subdominant topological term in the entanglement entropy of a subsystem (dubbed the topological entanglement entropy) [28–46] quantifies the long-ranged nature of the entanglement. This is in contrast to systems with local interactions whose subsystem entanglement entropy scales with the area of the boundary of the subsystem [3, 47, 48].

More pertinent to the present work is the entanglement of free (i.e., non-interacting) fermionic systems. Specifically, we will consider the case of relativistic Dirac fermions in two dimensions, both massless as well as massive. They are known to emerge in several condensed matter systems [49], appearing at the surfaces of three-dimensional topological insulators [50–53], quasi-2D organic materials [54–56] and in artificial quantum simulators such as cold atom gases, molecular

and microwave crystals [57–63]. For massless critical systems (or conformal field theories (CFTs)) living in one spatial dimension, the entanglement entropy (S) of a single subsystem of length l scales as $S \sim \frac{c}{3} \ln l$ [64–73], where c is the conformal central charge of the CFT. For massive fermions, an entropic c -function (spatial derivative of the entanglement entropy) can be expressed in the form of differential equations that need to be solved numerically [74–77]. The solutions for a single interval of length l lend themselves to small and large mass expansions, reducing to $S \sim \frac{1}{3} \ln \frac{l}{\epsilon} - \frac{1}{6} (ml \ln ml)^2 + O((ml)^2)$ for the case of small ml , and to $S \sim (ml)^{-1/2} e^{-2ml}$ for that of large ml . The $\ln l$ behaviour is a specific case of the more general $S \sim l^{d-1} \ln l$ violation of the area law observed in d -dimensional fermionic critical systems [74, 78–92]. This violation arises from the non-local nature of the gapless quantum fluctuations that lie proximate to the $d - 1$ -dimensional Fermi surface of a quantum critical fermionic system in d spatial dimensions.

While there is no geometry-independent subdominant term in the entanglement entropy of free fermionic systems [93, 94], it is possible to generate such a term by placing the system on a multiply connected manifold such as a cylinder, and inserting a magnetic flux through the cylinder [93, 95–98]. It has been shown that if there are ϕ number of electronic flux quanta piercing the system, an additional term is generated in the entanglement entropy of a subsystem of massless Dirac fermions of sufficiently large length (as defined in Ref. [93]) with the form $\frac{1}{6} \ln |2 \sin \frac{\phi}{2}|$ [93, 96]. Further, there is evidence from numerical computations on discrete models that such a term is a signature of the specific field theory and encodes universality [98–100]. In this work, we put this idea on a stronger analytical footing by relating the flux-dependent term to a topological invariant of the system of free fermions: the Luttinger volume [101–107].

Entanglement hierarchy and the holographic principle

In free fermion systems, the Lagrangian is diagonal in momentum space, and the entanglement mentioned above must arise purely from gapless quantum fluctuations in real space. Further, the modified area law behaviour of the entanglement entropy shows that the entanglement is long ranged in nature. This motivates us to investigate the dependence of the entanglement of a subsystem on its size in momentum space. We adopt a coarse-graining strategy in defining subsystems at various scales, and find that the entanglement entropy hence obtained has a Russian doll-like nested structure, i.e., increasing the size of the subsystem in momentum space gradually reveals a hierarchical arrangement of the entanglement. We interpret this scaling behaviour as the emergence of an additional dimension along a renormalisation group (RG) flow of the entanglement [108–110]. This allows us to define a measure of distance along the RG flow using a non-negative measure of entanglement such as the mutual information between successive coarse-graining scales [111–114]: the more the entanglement, the less will be the distance between those points.

The generation of an additional dimension along an RG flow of a system away from criticality is the essence of the AdS/CFT conjecture or, more generally, the holographic principle. The principle, also known as the gauge-gravity duality [115–122], posits that there exists a duality relation between a quantum field theory in d -spatial dimensions and a gravity theory in $d + 1$ -spatial dimensions [123–126]. There is now sufficient evidence that the additional dimension can be visualised as a renormalisation group flow that starts from the critical field theory on the boundary and extends into the bulk [127–136]. The most popular realisation of the holographic principle is the AdS/CFT correspondence that links a super-symmetric gauge theory with a string theory through a strong-weak duality relation [137–144]. More generally, the strong-weak duality enables studying a system with strong correlations by mapping onto a problem with weak (classical) gravity that can be solved using well-known methods [145, 146]. This has led to new insights in various areas of high energy and condensed matter physics, such as the viscosity of the quark-gluon plasma [147], the response functions of the Bose-Hubbard model [148, 149], and the phenomenology of non-Fermi liquids [150–153], holographic superconductors [154–159], striped phases [160–162] and holographic Fermi liquids [163–167]. An overview of the metallic states (i.e., phases that satisfy Luttinger’s theorem) and their connections to the gauge-gravity duality have been provided in Refs. [168–170].

Conversely, the holographic principle also implies that studying the boundary conformal theory can provide insights into the nature of the bulk quantum gravity theory. This requires constructing the emergent dimension from first principles by investigating the RG flow of the (often strongly coupled) quantum field theory, and has proved to be considerably more difficult. Nevertheless, there exist some examples of constructive attempts towards a bulk gravity theory [106, 107, 113, 114, 171–204]. Some notable attempts include the momentum-shell renormalisation approach of Refs.[184–187] and the multi-scale entanglement renormalisation ansatz (MERA) approach of Refs.[188–192]. Indeed, both approaches use certain forms of an RG flow to generate the extra spatial dimension: the former integrates out high momentum degrees of freedom in favour of generating dynamics for the boundary gauge field, with the RG trajectory variable giving rise to the additional spatial dimension [117, 184–187]. On the other hand, MERA works by disentangling degrees of freedom in real space, creating a tensor network in the process [193–195] and leading to a renormalisation in the many-particle entanglement that is interpreted as the additional dimension [190]. There exist other approaches that also proceed via entanglement renormalisation, such as the exact holographic mapping [113, 114] (EHM) and the unitary renormalisation group (URG) approach [106, 107, 196] that operate purely through unitary transformations and have been explicitly shown to lead to a holographic tensor network along the RG flow. Apart from these, a recent approach [197–199] has involved providing a geometric description of the Wilsonian renormalisation group [205, 206], creating thereby an RG framework in terms of an order-parameter field that extends the Ads/CFT correspondence to non-critical theories [200–204].

We extend this body of work by providing another explicit demonstration of the holographic principle in the form of a simple and tractable exact holographic mapping (EHM) for free fermion systems that yields analytic relations between the RG flow parameters and their dual bulk quantities such as distances and curvature. This is carried out by defining and implementing a scaling transformation on the set of k -states in the effective Hilbert space. Importantly, this method allows the generation of all three kinds of spaces - bounded, unbounded and flat. The work is divided into three main parts. In Sec. 2, we describe the system we work with, and define certain physical ideas and measures of entanglement that are employed in the later sections. In Sec. 3, we define the scaling transformations mentioned earlier, and discuss its implications on the scaling of entanglement in the system under study. In Sec. 4, we probe the holographic nature of the entanglement, unveiling an emergent spatial dimension in the process and obtain several characteristics of this emergent geometry. In Sec. 5, we probe the topological aspects of the entanglement, and discuss its implications for the system at hand. In Sec. 6, we summarise our results and briefly mention some open questions. For the convenience of the reader, we present below a summary of the main results obtained by us.

Summary of main results

- We devise a coarse graining scheme in k -space for a system of non-interacting fermions in two spatial dimensions, and show that the scaling of the entanglement entropy owing to the renormalisation group transformations reveals a hierarchical variation of the entanglement with scale. Computing multipartite measures of entanglement (entanglement between three modes, four modes and so on) reveals the same hierarchy, and we interpret the scaling of the entanglement as the emergence of an additional spatial dimension.
- We relate several parameters like distances and curvature of the additional dimension to an appropriately defined beta function of the RG flow, providing thereby an explicit analytic manifestation of the holographic principle. We find that the curvature can adopt all three signatures $(+, -, 0)$, depending on the value of the anomalous dimension corresponding to the RG flow of the spectral gap in the electronic dispersion. We show that a change in the sign of the curvature corresponds to a topological change in certain winding numbers.
- We show that the subdominant topological part of the entanglement is invariant under these scaling transformations for a system of fixed number density, and is related to the Luttinger volume of the gapless fermionic system. Upon placing the system in a perpendicular magnetic

field, we demonstrate that the topological invariant in the metallic state (Luttinger volume) transforms into a topological invariant on the insulating state (Chern numbers of the quantum hall state) as the magnetic field is tuned towards the regime of Landau levels.

- The entanglement hierarchy can be represented as a hypergraph corresponding to the emergent space. Considering only the mutual information reduces the hypergraph to a simple graph with 1–dimensional edges embedded in a metric space with a well-defined geodesic and metric dimension.

2 Preliminaries and definitions

2.1 The system

In this work, we focus on the case of Dirac fermions in two spatial dimensions described by the Lagrangian (in natural units $\hbar = c = 1$) $\mathcal{L} = \int dx dy \bar{\psi}(x, y, t) (i\gamma^\mu \partial_\mu - m) \psi(x, y, t)$. The system is placed on a 2–torus of dimensions $L_x \times L_y$ with periodic boundary conditions, such that $\psi(x, y, t) = \psi(x + L_x, y, t) = \psi(x, y + L_y, t)$. Entanglement measures will be calculated in the presence of a gauge field A that transforms the Lagrangian by shifting the momenta: $i\partial_\mu \rightarrow i\partial_\mu + eA$. We choose the vector potential A such that, in any particular setup, it couples to just one component of the momentum (say, the x –component). This results in $\phi = eAL_x/2\pi$ units of flux quantum threading the torus in the y –direction. One of our goals is to express the Luttinger volume V_L in terms of multi-partite measures of entanglement ($I_{\{\mathcal{A}_i\}}^g(\phi)$) between multiple subsystems $\{\mathcal{A}_i, i = 1, 2, \dots, g\}$ [207], in the presence of the flux ϕ . The precise definition of I^g and the method of choosing the subsystems will be given later. In order to calculate $I_{\{\mathcal{A}_i\}}^g$, however, we find it convenient to take the thin torus limit: $(L_y/L_x) \rightarrow \infty$, keeping l/L_y fixed. Importantly, this operation does not affect quantities such as V_L as long as we keep the number density unchanged.

In order to calculate entanglement measures, we will express the 2 + 1–dimensional system as a sum of an infinite number of massive 1 + 1–dimensional systems [92, 93, 96, 208]. In the presence of a gauge field $\vec{A} = A\hat{x}$, the complete Lagrangian (in natural units) is

$$\mathcal{L} = \int dx dy \bar{\psi}(x, y) [\gamma^\mu (i\partial_\mu + eA_\mu) - m] \psi(x, y) , \quad (2.1)$$

where $A_\mu = A\delta_{\mu,x}$ and $\phi = eAL_x/2\pi$. The integral ranges over the surface area of the torus, and the time dependence of the fields has been suppressed. Due to the periodic boundary conditions (PBCs) in the x –direction, the momenta k_x are quantised: $k_x^n = \frac{2\pi n}{L_x}, n \in \mathbb{Z}$. We then expand the fields $\psi(x, y)$ in these momenta:

$$\psi(x, y) = \sum_{n=-\infty}^{\infty} e^{ik_x^n x} \psi(k_x^n, y) . \quad (2.2)$$

In terms of these dual fields, the Lagrangian can be shown to be equivalent to a tower of massive 1 + 1–dimensional fermions (details are provided in Appendix A):

$$\mathcal{L} = \sum_{k_x^n} \int dy \bar{\psi}(k_x^n, y) (i\gamma^\mu \partial_\mu - M(n, \phi)) \psi(k_x^n, y) , \quad (2.3)$$

with an effective mass $M_{n,\phi}$ given by

$$M_{n,\phi} = \sqrt{m^2 + (k_x^n + eA)^2} = \sqrt{m^2 + \frac{4\pi^2}{L_x^2} (n + \phi)^2} . \quad (2.4)$$

This decoupling ensures that the various modes $n \in \mathbb{Z}$ are disentangled from one another, such that the total density matrix ρ_{2D} of the 2 + 1–dimensional system can be written as a product of the

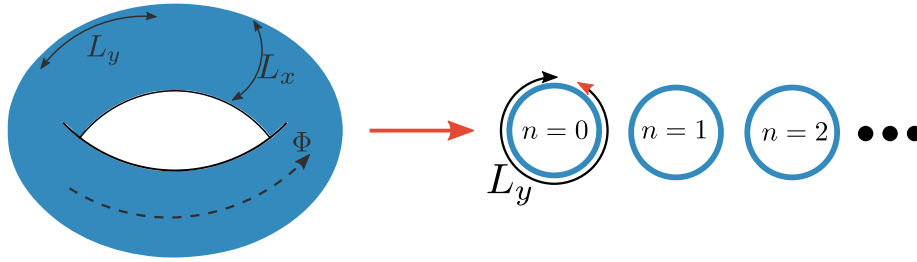


Figure 1. The 2 + 1–dimensional system of noninteracting electrons with periodic boundary conditions is mapped to a sum of 1 + 1–dimensional systems that are decoupled from each other. Each momentum quantum number k_x^n gives rise to a distinct 1 + 1–dimensional system.

density matrices ρ_{1D}^n for each of the modes:

$$\rho_{2D} = \prod_{n=-\infty}^{\infty} \rho_{1D}^n . \quad (2.5)$$

We will focus primarily on the case of massless 2 + 1–dimensional electrons by setting $m = 0$, such that the effective mass is given by $M_{n,\phi} = \frac{2\pi}{L_x} |n + \phi|$. Certain results will, however, be generalised to the case of massive fermions ($m \neq 0$). While the massless case corresponds to the gapless excitations of a Fermi liquid or those at the surface of a topological insulator, the massive case corresponds to gapped or insulating states of matter, e.g., the Bogoliubov-de Gennes quasiparticles above an s –wave superconducting gap. Massive Dirac fermions have also been observed experimentally in several materials like ultrathin films [209], topological insulating crystals [210] and van der Waals heterostructures [211]. They are also emergent at low-energies, for instance, in fermionic nonlinear σ –models [212], and can also be realised near the IR fixed point of the kagome Heisenberg quantum antiferromagnets placed in an external magnetic field along the z –direction [213].

2.2 Entanglement measures

We will work with two measures of entanglement discussed below. Given the density matrix $\rho = |\Psi\rangle\langle\Psi|$ for the ground state $|\Psi\rangle$ of the complete system, the entanglement entropy (EE) of a set of subsystems $\{\mathcal{A}_i, i = 1, 2, \dots, g\}$ with the rest of the system is given by:

$$S_{\{\mathcal{A}_i\}} = -\text{Tr} [\rho_{\{\mathcal{A}_i\}} \ln \rho_{\{\mathcal{A}_i\}}] ; \quad \rho_{\{\mathcal{A}_i\}} = \text{Tr}_{\{\mathcal{A}_i\}} [\rho] . \quad (2.6)$$

$\text{Tr}[\cdot]$ is the trace operation over all degrees of freedom, while $\text{Tr}_{\{\mathcal{A}_i\}}[\cdot]$ is the partial trace over only the states corresponding to the set of subsystems $\{\mathcal{A}_i\}$. $\rho_{\{\mathcal{A}_i\}}$ is referred to as the reduced density matrix for the rest of the system (complement of the set $\{\mathcal{A}_i\}$). Using EE, one can define the mutual information $I(\{\mathcal{A}_i\} : \{\mathcal{B}_i\})$ between two subsystems A and B :

$$I_2(\{\mathcal{A}_i\} : \{\mathcal{B}_i\}) = S(\{\mathcal{A}_i\}) + S(\{\mathcal{B}_i\}) - S(\{\mathcal{A}_i\} \cup \{\mathcal{B}_i\}) , \quad (2.7)$$

where $S(\{\mathcal{A}_i\} \cup \{\mathcal{B}_i\})$ is the EE of $\{\mathcal{A}_i\} \cup \{\mathcal{B}_i\}$ with the rest. Higher order measures of information among N subsystems can also be defined similarly (see, e.g., [207]). Such multi-partite measures of quantum information convey the degree of correlations present within the system - the presence of N –particle correlations ensures all information measures up to the N –partite information will be non-zero.

2.3 Luttinger volume

The Luttinger volume V_L is defined as the number of \vec{k} –space points inside the Fermi surface [101, 102] :

$$V_L = \int_{G(\omega=0, \vec{k})} \frac{1}{(2\pi)^d} d\vec{k} . \quad (2.8)$$

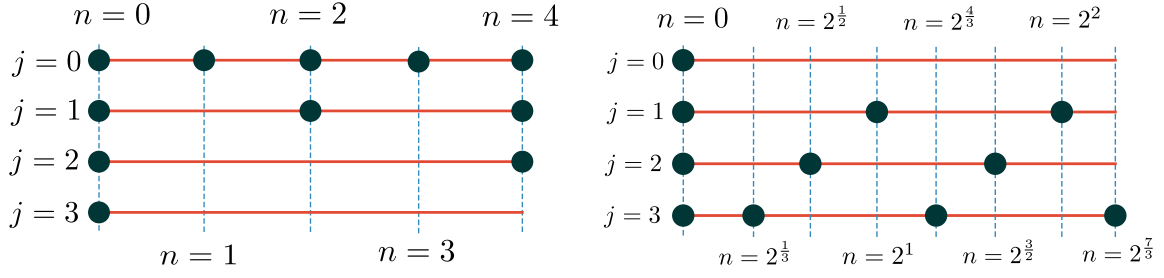


Figure 2. *Left:* Coarse-graining of k_x -states for $z > 0$. *Right:* Fine graining of states for $z < 0$.

The integral runs over all \vec{k} -space points where the $\omega = 0$ Greens function is positive, and the Fermi surface is defined as the set of points in \vec{k} -space where $G(\omega = 0, \vec{k})$ changes sign. This quantity can be related to a topological winding number that counts the number of poles and zeros in the Greens function [104], and responds to a flux that pierces the system [103]. For gapless systems, V_L is equal to the average number density of electrons in the system, leading to Luttinger's theorem [101–107]. This theorem states that the Luttinger volume at $T = 0$ is preserved upon the adiabatic introduction of electronic interactions (as long as the system does not undergo a quantum phase transition).

3 Entanglement hierarchy in mixed momentum and real space

Before beginning our calculations of entanglement measures, we define the subsystem(s) whose entanglement we want to obtain. The subsystems we will use in this work are of the following kind:

$$\mathcal{A}_{i,z} = \tilde{A}_{i,z} \times A_{i,z} , \quad (3.1)$$

where i takes integral values starting from zero, z can take all integral values apart from 0 and \times represents the Cartesian product between the set of real space points $\tilde{A}_{i,z} = \{0 \leq y \leq l\}$ and the set of momentum space points

$$A_{i,z} = \left\{ k_x^n \right\}; \quad k_x^n = \frac{2\pi}{L_x} n; \quad \max(\{k_x^n\}) = \frac{2\pi N}{L_x} ; \\ n \in \{-N, -N + t_z(i), \dots, -t_z(i), 0, t_z(i), N\}; \quad t_z(i) = 2^{i^z} , \quad (3.2)$$

and where $t_z(i) = 2^{i^z}$ is the difference between consecutive values of n .

The subset $\mathcal{A}_{i,z}$ is therefore a region in mixed momentum and real spaces, spanned by the variables k_x and y respectively. In y -space, the region is of length l and bounded by the points $y = 0$ and $y = l$. In k_x -space, $\mathcal{A}_{i,z}$ comprises the points $\left\{ 0, \pm 2^{i^z} \frac{2\pi}{L_x}, \pm 2^{i^z} \frac{4\pi}{L_x}, \dots \right\}$ such that $|k_x| \leq \frac{2\pi N}{L_x}$. For example, for the case of $z = 1$ and N being a multiple of 4, we have

$$A_{0,1} = \left[-\frac{2\pi}{L_x} N, -\frac{2\pi}{L_x} (N-1), \dots, -\frac{2\pi}{L_x} 2, -\frac{2\pi}{L_x} 1, 0, \frac{2\pi}{L_x} 1, \frac{2\pi}{L_x} 2, \dots, \frac{2\pi}{L_x} (N-1), \frac{2\pi}{L_x} N \right] , \\ A_{1,1} = \left[-\frac{2\pi}{L_x} N, -\frac{2\pi}{L_x} (N-2), \dots, -\frac{2\pi}{L_x} 4, -\frac{2\pi}{L_x} 2, 0, \frac{2\pi}{L_x} 2, \frac{2\pi}{L_x} 4, \dots, \frac{2\pi}{L_x} (N-2), \frac{2\pi}{L_x} N \right] , \quad (3.3) \\ A_{2,1} = \left[-\frac{2\pi}{L_x} N, -\frac{2\pi}{L_x} (N-4), \dots, -\frac{2\pi}{L_x} 8, -\frac{2\pi}{L_x} 4, 0, \frac{2\pi}{L_x} 4, \frac{2\pi}{L_x} 8, \dots, \frac{2\pi}{L_x} (N-4), \frac{2\pi}{L_x} N \right] .$$

Note that N represents the edge of the Brillouin zone, and will be sent to infinity when we calculate quantities in the continuum limit.

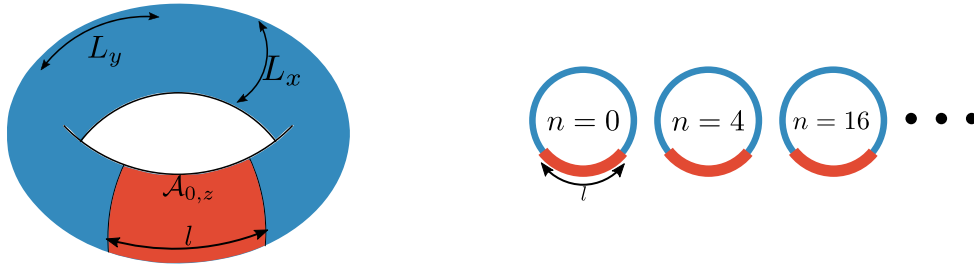


Figure 3. *Left:* Setting $i = 0$ leads to unchanged length L_x along x and the constraint $0 \leq y \leq l$ in the y -direction. This creates an annulus (red region) of height l and circumference L_x . *Right:* Typical members of the set $\mathcal{A}_{i,z}$ for $i = 2, z = 1$.

We note here that the transformations for $z < 0$ correspond to increasing the density (finer-graining) of k_x -states by adding more momentum states while keeping the bounds fixed. This involves reducing the interval in k_x -space, and hence equivalent to increasing the system size L_x . This is similar to methods such as numerical renormalisation group treatment of the Kondo problem [205] where an increasing number of states are added to the system at increasingly larger distances from the impurity site, such that the system asymptotically goes to the thermodynamic limit. The other case of $z > 0$ is, on the contrary, a decimation process in k_x -space, and equivalent to reducing the system size. Indeed, it will be shown later that the sequence of Hamiltonians generated in the process (for both positive and negative z) are related to one other by renormalisation group transformations.

Within a given set $\mathcal{A}_{i,z}$, the distance between adjacent k -space points is $\frac{2\pi}{L_x} t_z(i)$ where $t_z(i) = 2^{i^z}$. Choosing $i = 0$ keeps the set of k_x -space points unchanged, such that we recover the entire Lagrangian of eq. (2.1) in the x -direction for system size L_x , while the y -direction is constrained to length l . This means that \mathcal{A}_0^z is actually just an annulus that wraps around the x -direction of the torus and extends to a length l longitudinally in the y -direction (shown in Fig. 3). Along with the period $t_z(i)$, one can also define the fraction of maximum points present in the set $\mathcal{A}_{i,z}$ as

$$f_{i,z} = 1/t_z(i) = 2^{-i^z}. \quad (3.4)$$

For example, for $z > 0$, $f_{i,z} = 2^{-i^z}$ expresses the fact that in going from the set at $j = 0$ to the set at $j = i$, the number of elements in the set is scaled down by a factor of 2^{i^z} (see Fig. 4).

We now define the shorthand notation $S_{i,z}(\phi) \equiv S_{\mathcal{A}_{i,z}}(\phi)$ to denote the EE of the subsystem $\mathcal{A}_{i,z}$ in the presence of the Aharonov-Bohm flux ϕ . In order to calculate $S_{i,z}$, we start with $i = 0$. As mentioned earlier, this is essentially the EE between an annulus of length l and the rest of the 2-torus. Since the density matrices are in product, the total EE is just a sum of the EE arising from each mode:

$$S_{\mathcal{A}_{0,z}}(\phi) \equiv S_{0,z}(\phi) = \lim_{N \rightarrow \infty} \sum_{n=-N}^N S_{\tilde{\mathcal{A}}_{0,z}}^n, \quad (3.5)$$

where $\tilde{\mathcal{A}}_{0,z}$ acts as a projection of the annulus on the $k_x - y$ plane, and S^n indicates that the EE is calculated for the n^{th} mode. Each massive fermionic mode has a correlation length-scale $\xi_n = 1/M_{n,\phi}$. We choose l to be much larger than the largest correlation length: $l \gg \max(\{\xi_n, \forall n\})$. Using the expression for ϕ and the quantisation of the momenta k_x^n , this condition can be expressed as

$$l \gg \frac{L_x}{2\pi} \times \max\left(\left\{\frac{1}{|n + \phi|}\right\}\right) = \frac{L_x}{2\pi \{\phi\}}, \quad (3.6)$$

where $\{\phi\} = \phi - \lfloor \phi \rfloor$ is the fractional part of the flux ϕ in units of the flux quantum. Since we are in the thin torus limit, L_x must remain finite, and the maximum correlation can diverge only if $\{\phi\} = 0$. We ensure that l is larger than the correlation lengths by choosing ϕ to be necessarily non-integral, as this guarantees that the correlation lengths remain finite. Then, the EE of the

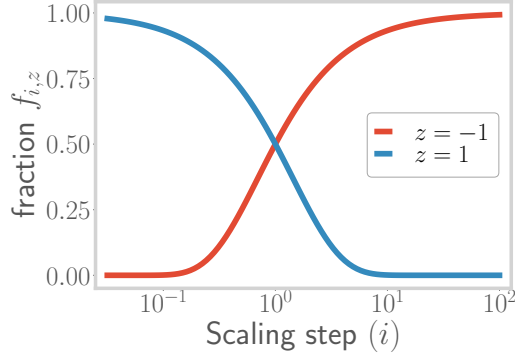


Figure 4. Fraction of the initial states present in the subsystem at various stages i . This fraction decreases for $z > 0$ (blue curve), and increases for $z < 0$ (red curve).

annulus is given by [93, 96]

$$S_{0,z}(\phi) = c \left[\alpha \frac{L_x}{\epsilon} - \ln |2 \sin(\pi\phi)| \right], \quad (3.7)$$

where c is the conformal central charge and ϵ is a UV cutoff; c is $1/3$ for a Dirac fermion. The computation of $S_{0,z}(\phi)$ uses the EE $S_{A_{0,z}}^n$ of a 1-D chain of fermions with a mass $M_{n,\phi}$ [71, 78]: $S_{A_{0,z}}^n = c \ln \frac{L_x}{2\pi\epsilon} - c \ln |n + \phi|$. On summing over n and regularising the UV cutoff, the first term of eq.(3.7) produces the leading area-law term of $S_0(\phi)$ [93]:

$$\sum_{n=-\infty}^{\infty} c \ln \frac{L_x}{2\pi\epsilon} \rightarrow c\alpha \frac{L_x}{\epsilon}, \quad (3.8)$$

where α is a cutoff-dependent non-universal constant. The flux-dependent term in $S_{A_{0,z}}^n$ leads to the sub-leading term of $S_{0,z}(\phi)$, and requires a regularisation using the Hurwitz zeta function [93]:

$$\sum_{n=-\infty}^{\infty} \ln |n + \phi| = \sum_{n=-\infty}^{\infty} [\ln |n + \phi| + \ln |n + (1 - \phi)|] = -\frac{\partial\zeta(\phi)}{\partial\phi} - \frac{\partial\zeta(1 - \phi)}{\partial\phi}, \quad (3.9)$$

where $\zeta(\phi) = \sum_{n=-\infty}^{\infty} (n + \phi)^{-1}$ is the Hurwitz zeta function. The derivative converges to $\frac{\partial\zeta(\phi)}{\partial\phi} = \ln \Gamma(\phi) - \frac{1}{2} \ln 2\pi$, as long as the zero mode $n + \phi = 0$ is excluded from the summation. The latter condition is guaranteed as we have chosen ϕ to be a non-integer. Γ is the Gamma function, satisfying $\Gamma(\phi)\Gamma(1 - \phi) = \pi / \sin(\pi\phi)$. Substituting the derivative gives [93, 96, 100]

$$\sum_{n=-\infty}^{\infty} \ln |n + \phi| = \ln 2\pi - \ln [\Gamma(\phi)\Gamma(1 - \phi)] = \ln |2 \sin(\pi\phi)|. \quad (3.10)$$

For a general $\mathcal{A}_{i,z}$, there are certain modifications to the expression in Eq. (3.7). For the first term in eq.(3.7), we have

$$\lim_{N \rightarrow \infty} \sum_{\substack{n=-N, \\ -N+t_z(i), \dots}}^N c \ln \frac{L_x}{2\pi\epsilon} = \lim_{N \rightarrow \infty} \sum_{\substack{n'=-\frac{N}{t_z(i)}, \\ -\frac{N}{t_z(i)}+1, \dots}}^{\frac{N}{t_z(i)}} c \ln \frac{L_x}{2\pi\epsilon} = t_z^{-1}(i) \lim_{N \rightarrow \infty} \sum_{n=-N}^N c \ln \frac{L_x}{2\pi\epsilon} \rightarrow c f_{i,z} \frac{\alpha L_x}{\epsilon}. \quad (3.11)$$

Similarly, for the second term, we have

$$\begin{aligned} \lim_{N \rightarrow \infty} \sum_{\substack{n=-N, \\ -N+t_z(i), \dots}}^N \ln |n + \phi| &= \lim_{N \rightarrow \infty} \sum_{\substack{n'=-\frac{N}{t_z(i)}, \\ -\frac{N}{t_z(i)}+1, \dots}}^{\frac{N}{t_z(i)}} \ln |n' t_z(i) + \phi| = \lim_{N \rightarrow \infty} \sum_{\substack{n'=-\frac{N}{t_z(i)}, \\ -\frac{N}{t_z(i)}+1, \dots}}^{\frac{N}{t_z(i)}} \ln (f_{i,z} |n' + f_{i,z} \phi|) \\ &= \sum_{n'=-\infty}^{\infty} \ln |n' + f_{i,z} \phi|, \end{aligned} \quad (3.12)$$

where we have assumed that $t_z(i)$ is finite, and dropped the constant part $\ln f_{i,z}$ (which can be absorbed into the UV cutoff ϵ in eq. (3.11)). Following Eq. (3.10), this gives

$$\lim_{N \rightarrow \infty} \sum_{\substack{n=-N, \\ -N+t_z(i), \dots}}^N \ln |n + \phi| = \ln |2 \sin(\pi f_{i,z} \phi)|. \quad (3.13)$$

Combining both parts, we obtain the expression for the EE that will be employed in what lies ahead:

$$S_{i,z}(\phi) = c f_{i,z} \frac{\alpha L_x}{\epsilon} - c \ln |2 \sin(\pi f_{i,z} \phi)|. \quad (3.14)$$

It is evident from the expression in eq. (3.14) that, as modes are added into the subsystem, the L_x -dependent geometric part of the EE increases, leading to a *hierarchical structure* in the entanglement. A similar result was previously shown to hold for geometric measures of entanglement of quantum-mechanical systems with eigenstates such as the W and GHZ states and their symmetric superpositions [214]. The variation of the geometric part with the subsystem index j is shown in Fig. 4.

The above-mentioned hierarchy in entanglement measures leads to an interesting property for the entanglement: the combined entanglement entropy of any number of systems $\{\mathcal{A}_{i,z}\}$ is equal to the entanglement entropy of the most dense system among them. For $z > 0$, the sets become smaller as the RG index increases, while for $z < 0$, the sets become larger as the RG index increases. Thus, we may write

$$S_{\{\mathcal{A}_{i,z}\}} = \theta(z) S_{\min\{i\},z} + \theta(-z) S_{\max\{i\},z}. \quad (3.15)$$

The mutual information $I^2(i, j)$ between the systems at two RG steps i and j can then be computed:

$$I^2(i, j) \equiv S_{i,z} + S_{j,z} - S_{i \cup j, z} = \theta(-z) S_{\min(i,j),z} + \theta(z) S_{\max(i,j),z}. \quad (3.16)$$

In light of this subsystem-based hierarchical structure, we can also consider the g -partite information $I_{\{\mathcal{A}_{i,z}\}}^g$ among g sets $\{\mathcal{A}_{i,z}\}$. I^g is defined as [207]

$$I_{\{\mathcal{A}_{i,z}\}}^g = \sum_{r=1}^g (-1)^{r+1} \sum_{\substack{\beta \in \mathcal{P}(\{\mathcal{A}_{i,z}\}) \\ |\beta|=r}} S_{\beta}, \quad (3.17)$$

where $\mathcal{P}(\{\mathcal{A}_{i,z}\})$ is the power set of $\{\mathcal{A}_{i,z}\}$, and $|\beta| = r$ indicates that the sum is carried out only over those sets β that have r number of elements in them. For example, for $g = 3$, we have

$$I^3 = S_{\mathcal{A}_{0,z}} + S_{\mathcal{A}_{1,z}} + S_{\mathcal{A}_{2,z}} - S_{\mathcal{A}_{0,z} \cup \mathcal{A}_{1,z}} - S_{\mathcal{A}_{1,z} \cup \mathcal{A}_{2,z}} - S_{\mathcal{A}_{2,z} \cup \mathcal{A}_{0,z}} + S_{\mathcal{A}_{0,z} \cup \mathcal{A}_{1,z} \cup \mathcal{A}_{2,z}}. \quad (3.18)$$

For our choice of subsystems, the g -partite information can be shown to be equal to the EE of the *intersection set* of the concerned g -sets (details in Appendix B). For the case of $z > 0$, this takes the form

$$I_{\{\mathcal{A}_{i,z}\}}^g(\phi) = S_g(\phi) = c f_{g,z} \alpha \frac{L_x}{\epsilon} - c \ln |2 \sin(\pi f_{g,z} \phi)|. \quad (3.19)$$

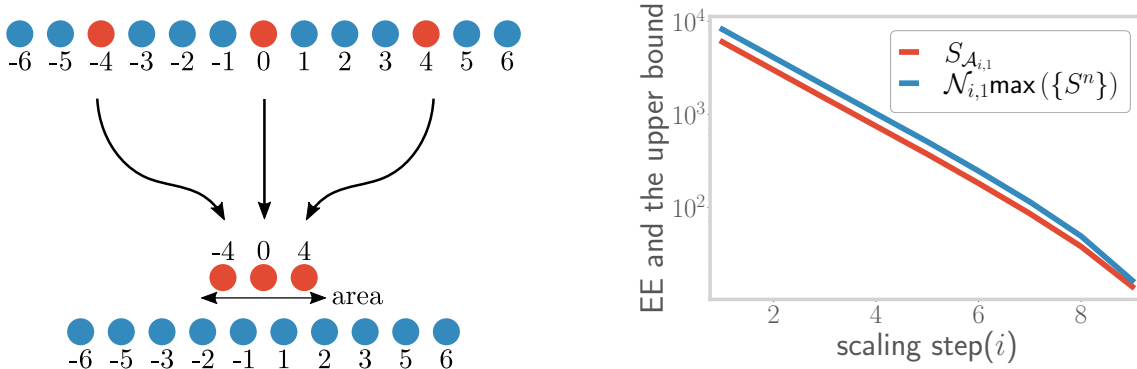


Figure 5. *Left:* Modes forming the subsystem $\mathcal{A}_{i,z}$ (red circles) form the boundary between $\mathcal{A}_{i,z}$ and its complement (blue circles). *Right:* Scaling of the subsystem entanglement entropy (red), and its upper bound (blue), as the RG transformations are performed (denoted by increasing index i). The bound is saturated at large i .

Since the g -partite information is simply the EE of the g^{th} subsystem, the hierarchy in the EE can thus be seen to lead to multiple levels of correlation in the system, corresponding to an increasing number of parties entering the set.

Finally, we note that the geometric (L_x -dependent) part of the EE in eq. (3.14), as well as any of the information measures I^g (eq. (3.19)), has the same form even if we start with a non-zero mass $m > 0$ [93]. This ensures that the above observations regarding the hierarchical structure of the entanglement hold even for gapped electronic systems.

4 Holographic geometry of the RG flow

4.1 EHM and the Ryu-Takayanagi bound for the gapless and gapped cases

As we will now show, the approach laid out above to the creation of subsystems amounts essentially to performing a sequence of renormalisation group (RG) transformations on the momentum modes of the Hamiltonian in the x -direction. We consider here the general case of massive Dirac electrons $M_{n,\phi} = \sqrt{m^2 + \frac{\pi^2}{L_x^2} (n + \phi)^2}$. Further, we define the superset $\mathcal{A}_z^{(0)}$ of k_x -states: $\mathcal{A}_z^{(0)} = \bigcup_{i=0}^{\infty} \mathcal{A}_{i,z}$, such that all k_x -states that can appear at any point of the sequence $\{\mathcal{A}_{i,z}; i = 0, 1, 2, \dots\}$ are present within it. This superset can now be used to define a parent Hamiltonian \mathcal{H}_0 that consists of all the modes in the x -direction:

$$\mathcal{H}^{(0)} = \sum_{k_x \in \mathcal{A}_z^{(0)}} \mathcal{H}(k_x), \quad (4.1)$$

where $\mathcal{H}(k_x)$ is the Hamiltonian for a massive Dirac fermion that extends over a length L_y in the single spatial dimension, and having mass $M_{n,\phi}$. The Hamiltonian at any given step of the RG is then obtained by projecting onto appropriate sets of momenta. The set of momentum at step j is given by $\mathcal{A}_{j,z} = \frac{2\pi}{L_x} \times \{0, \pm t_z(j), \pm 2t_z(j), \dots\}$ with $t_z(j) = 2^{jz}$. The projector onto this set is given by

$$P_{j,z} = \sum_{k_x^1=0,1} \sum_{k_x^2=0,1} \dots \sum_{k_x^N=0,1} |\hat{n}_{k_x^1} \hat{n}_{k_x^2} \dots\rangle \langle \hat{n}_{k_x^1} \hat{n}_{k_x^2} \dots|, k_x^j \in \mathcal{A}_{j,z}, \quad (4.2)$$

and the Hamiltonian at the corresponding step is then obtained as

$$\mathcal{H}_{i,z} = P_{i,z} \mathcal{H}^{(0)} P_{i,z}. \quad (4.3)$$

In this formulation of the RG, the index i represents the RG step, while the parameter z indicates the *strength of the scaling* mechanism: for $z > 0$, a higher value of z means that the states of the Hamiltonian become rarer as the index i increases, while for $z < 0$, the states become denser with increasing i . Importantly, we will see subsequently that the parameter z corresponds also to the anomalous dimension of the coupling that leads to a spectral gap in the electronic dispersion, dictating its growth or decay under RG evolution (eq.(4.12)).

Since this is a free theory, the k -modes are decoupled, and the projection operation preserves the spectrum of the remaining degrees of freedom. The renormalised Hamiltonian (eq. (4.3)) can then be said to constitute an exact holographic mapping (EHM) [113, 114] in the direction of the RG transformations. It is also pertinent to note that the sequence of transformations in eq. (4.3) can be thought of as a simple and specific example of a unitary renormalisation group (URG) procedure [106, 107] that first disentangles and then projects out a certain set of degrees of freedom. Because the operation is unitary, the URG preserves the spectrum in the process. In the present case, the disentanglement operation is unity. The URG has already been shown to lead to a holographic renormalisation of the Hilbert space geometry which can be seen through the evolution of the Fubini-Study metric under the URG transformations [106].

More evidence for the holographic nature of the construction comes from the fact that the entanglement entropy for both the massless and massive cases satisfy the bound provided by the Ryu-Takayanagi proposal that relates the entanglement of a conformal field theory (CFT) with the geometry of its gravity dual [143, 144]:

$$S_{\mathcal{A}_{i,z}} \leq \mathcal{N}_{i,z} \max(\{S^n\}) . \quad (4.4)$$

In the above constraint, $\max(\{S^n\})$ is the maximum single entropy of all the modes n residing in $\mathcal{A}_{i,z}$, and \mathcal{N} is the area of the minimal surface that separates the subsystem $\mathcal{A}_{i,z}$ from the rest. In order to see how this is satisfied in the present case, we note that since the subsystem $\mathcal{A}_{i,z}$ is interspersed among the rest of the system (see left panel of Fig. 5), the minimal surface is as large as the subsystem itself. The area of this surface is therefore given by the number of modes in $\mathcal{A}_{i,z}$. Using this information, the right hand side of eq. (4.4) can be written as

$$\mathcal{N}_{i,z} \max(\{S^n\}) = \max(\{S^n\}) N_{f_{i,z}} = \max(\{S^n\}) \sum_{n \in \mathcal{A}_{i,z}} . \quad (4.5)$$

Following Eq. (2.5), the left hand side of Eq. (4.4) can, on the other hand, be written as

$$S_{\mathcal{A}_{i,z}} = \sum_{n' \in \mathcal{A}_{i,z}} S^{n'} \leq \sum_{n' \in \mathcal{A}_{i,z}} \max(\{S^n\}) . \quad (4.6)$$

Comparing eqs. (4.5) and (4.6), we recover the Ryu-Takayanagi condition of eq. (4.4). The scaling of both the left and right hand sides of Eq. (4.4) has been shown in the right panel of Fig. 5.

Since the UV theory is already quadratic in the fields, there are no correlations between these modes. This raises the question on what precisely is being renormalised? There are three equivalent ways of looking at this. The first is to use eqs. (3.14) and (3.19) to interpret the RG flow as a renormalisation of the entanglement and multipartite information content in the system. The second is to think of the RG transformations as a flow in the spectral spacing parameter $M(n+1, \phi) - M(n, \phi)$: moving along the RG flow leads to an increase or decrease in the spacing between adjacent members of the spectrum. Finally, the third is to realise that the quantum fluctuations of this system of non-interacting electrons exist in real space, and the RG transformations simply serve to renormalise these fluctuations by decoupling certain k_x -modes.

4.2 RG evolution as the emergent dimension

To obtain a more specific description of the RG flow as the emergence of a geometric space, we introduce a measure of distance. For this, we will employ another bipartite measure of entanglement - the mutual information I^2 , as defined in eq. (2.7), due to its non-negative nature. We focus on

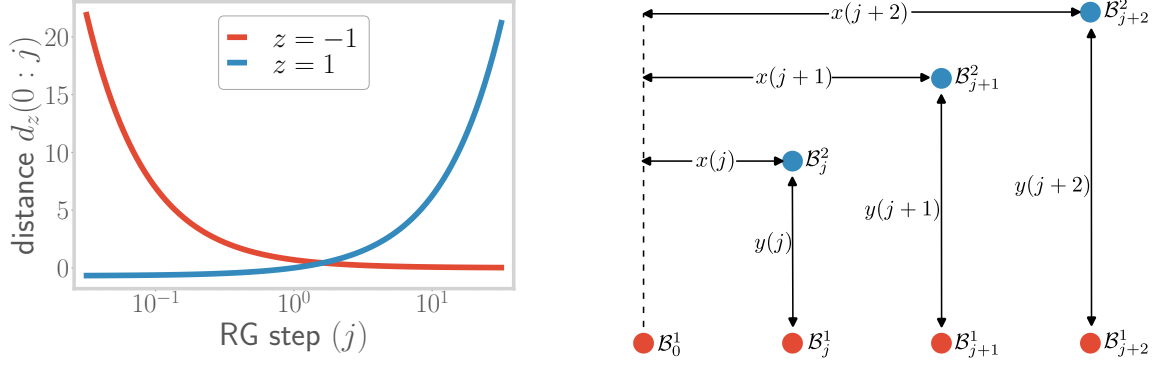


Figure 6. *Left:* Variation of the information distance $d_z(0 : j)$ (defined along the RG direction) under the decimation procedure. The $z = 1$ case shows linear increase while the $z > 1$ case shows super-linear increase. *Right:* Geometry of subsystems used for calculating the emergent curvature.

the massless case $m = 0$ for the time-being. Inspired by Refs. [111, 114, 215, 216], we adopt the following definition for distance:

$$d_z(i, j) \equiv \ln \frac{I_{\max}^2}{I_z^2(i : j)}, \quad (4.7)$$

where $I_z^2(i : j) \equiv I^2(\mathcal{A}_{i,z}, \mathcal{A}_{j,z})$ is the mutual information between the two mentioned sets, and I_{\max}^2 is the mutual information between two maximally entangled systems. Accordingly, $d_z(j)$ is zero (i.e., the mutual information is maximum) at $j = 0$ if $z > 0$ and $j = \infty$ if $z < 0$, and this distance increases (decreases) with the decrease (increase) in the mutual information as the scaling transformations are performed.

we compute the distance between the points i and j to obtain the scaling of the distance $d_z(j)$. We assume $i < j$ without loss of generality. At each step, we tune the flux ϕ so as to remove the flux-dependent part from the EE. Following eq. (3.16), the mutual information is of the form $\theta(-z)S_i + \theta(z)S_j$, such that the distance is given by

$$d_z(i, j) = \theta(-z) \ln \frac{S_{\max}}{S_{i,z}} + \theta(z) \ln \frac{S_{\max}}{S_{j,z}} = \theta(z)j^z \ln 2 + \theta(-z)i^z \ln 2. \quad (4.8)$$

For $z > 0$, the distance increases as j increases (keeping i fixed), as the k -space points are made more coarse-grained under the RG transformations. On the other hand, for $z < 0$, the distance decreases as i is increased (keeping j fixed). The rate of increase or decrease depends on the value of z . This scaling of the distance is shown in the left panel of Fig. 6.

At any given RG step j , we define two subsystems \mathcal{B}_j^1 and \mathcal{B}_j^2 . The first subsystem \mathcal{B}_j^1 is the entire set of states $\mathcal{A}_{j,z}$ available at the j^{th} RG step, while the second subsystem \mathcal{B}_j^2 is the set comprising those modes that remain to be considered at the next RG step if $z > 0$, and the set comprising only the modes that were present in the previous step for $z < 0$. This scheme is shown in the right panel of Fig. 6. The mutual information between these two sets defines a measure of distance y_j at the j^{th} RG step:

$$y_z(j) \equiv \ln \frac{I_{\max}^2}{I_z^2(\mathcal{B}_j^1 : \mathcal{B}_j^2)} = \begin{cases} (j+1)^z \ln 2, & z > 0, \\ (j-1)^z \ln 2, & z < 0. \end{cases} \quad (4.9)$$

The distance along the RG direction ($x_z(j)$) is, on the other hand, defined as the distance between the current RG step and the one with the maximum entanglement entropy:

$$x_z(j) \equiv \theta(z)d(0, j) + \theta(-z)d(j, \infty) = j^z \ln 2, \quad (4.10)$$

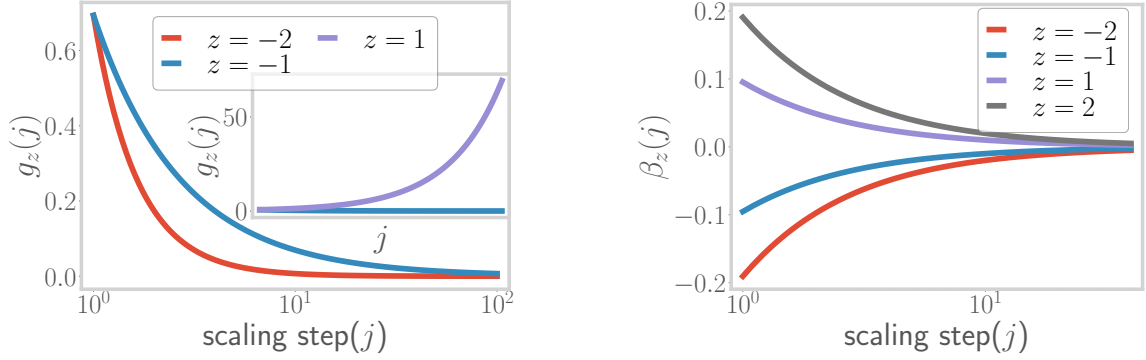


Figure 7. *Left:* Variation of coupling $g_z(j)$ under the scaling transformations, showing the irrelevance for $z < 0$ and relevance for $z > 0$ (inset). *Right:* Variation of RG beta function $\beta_z(j)$ for the coupling $g_z(j)$ with step index j . Fixed points are reached at $j \rightarrow \infty$.

where $d(i, j)$ was defined in eq. (4.7).

The connection of the x - and y -distances to the RG can be made manifest by relating them to the RG beta function. As we have seen above, even though we are working with massless Dirac fermions ($m = 0$), the Aharonov-Bohm flux and the dimensional reduction into $1 + 1$ -dimensional modes generate an effective mass $M_{n,\phi} = \frac{2\pi}{L_x}(n + \phi)$ for $n > 0$. At a specific RG step j , the n^{th} mode is given by $t_z(j) \times n$ on account of the RG transformations in k_x -space. With these points in mind, we define a coupling $g_z(j)$ that acts as a measure of the gap in the single-particle spectrum

$$g_z(j) \equiv \ln \frac{M_{n+1,\phi}(j) - M_{n,\phi}(j)}{2\pi/L_x} = \ln t_z(j) = j^z \ln 2. \quad (4.11)$$

The RG beta-function for the coupling $g_z(j)$ can then be written as

$$\beta_z(j) \equiv \frac{\Delta \log g_z}{\Delta j} = \log \frac{g_z(j+1)}{g_z(j)} = z \ln \left(1 + \frac{1}{j} \right), \quad (4.12)$$

where we have substituted $\Delta j = 1$. The beta function is positive for $z > 0$, indicating that the coupling $g_z(j)$ is RG-relevant in this regime (left panel of Fig. 7). On the other hand, the beta function is negative for $z < 0$, leading to irrelevant RG flows in this regime. The RG beta-function $\beta_z(j)$ itself decreases monotonically as j increases under the RG transformations (see Fig. 7): for a finite z , a fixed point is reached at $j \rightarrow \infty$ where the beta function goes to zero.

As we will now see, the flow of the RG beta functions can be related to the extremisation of a potential defined in the space of Hamiltonians. This potential is a function of the mutual information $I_z^2(0 : j)$:

$$\beta_z(j) = -\Delta \left[\ln \left(\ln \frac{I_z^2(0 : j)}{I_{\max}^2} \right) \right]. \quad (4.13)$$

The potential given within the square brackets above corresponds to an RG monotone whose fixed point corresponds with the fixed point of the RG. For relevant flows, the above equation ensures that the function $\ln \left(\ln \frac{I_z^2(0:j)}{I_{\max}^2} \right)$ is always minimised under the RG flow, with the consequence that the trajectories ultimately lead to minimisation of the mutual information. This indicates that the relevance of the mass coupling leads in turn to the decrease of the correlation length and hence a lowering of entanglement between points that are separated in real space. On the other hand, for irrelevant flows, the above-mentioned function is maximised, implying that the RG trajectories now maximise the entanglement. This reflects the fact that the decreasing mass leads to increased correlation lengths and an approach towards criticality.

Given eqs.(4.9), (4.10) and (4.13), we can relate the distances x and y to the beta function β_z :

$$x_z = \left(e^{\frac{\beta_z}{z}} - 1 \right)^{-z} \ln 2, \quad (4.14)$$

$$y_z = \begin{cases} x_z e^{\beta} & z > 0, \\ x_z \left(2 - e^{\frac{\beta}{z}} \right)^z & z < 0. \end{cases} \quad (4.15)$$

The contrasting behaviour of the beta function depending on the sign of z indicates that it tracks the effective number of degrees of freedom that contribute to the entanglement (eq. (3.14)) at any given RG step. Indeed, we find that the effective number of degrees of freedom is the effective c -function (or central charge) $\tilde{c}_z(j)$ of the theory, taking the form $\tilde{c}_z(j) = f_{i,z}c$. The beta function is thus related to the c -function as

$$\beta_z = \Delta \left[\ln \left(\ln \frac{c}{\tilde{c}_z(j)} \right) \right]. \quad (4.16)$$

For RG relevant flows, the c -function is found to diminish from the free fermion central charge $c = 1/3$, reaching the value of zero at the fixed point (where only the central $n = 0$ mode remains and the rest have been removed because of the large mass gap). The non-negative, non-increasing nature of the c -function, and its flow towards its minimum at the fixed point, leads to speculate that eq.(4.16) can be thought of as a holographic counterpart of Zamalodchikov's c -theorem [128, 217–219]. For RG irrelevant flows, the behaviour is reversed. The flow of the c -function is shown in the left panel of Fig. 8.

4.3 Curvature of the emergent space

Further insight on the spatial geometry of the RG flows can be obtained by looking at the curvature generated by the RG transformations. In the plane of the directions x and y generated by the RG flow, the curvature can be written as

$$\kappa_z(j) = \frac{v'_z(j)}{[1 + v_z(j)^2]^{\frac{3}{2}}}, \quad (4.17)$$

where

$$v_z(j) \equiv \frac{\Delta y_z(j)}{\Delta x_z(j)} = \frac{y_z(j+1) - y_z(j)}{x_z(j+1) - x_z(j)} = \begin{cases} \frac{(j+2)^z - (j+1)^z}{(j+1)^z - j^z} & z > 0, \\ \frac{(j)^z - (j-1)^z}{(j+1)^z - j^z} & z < 0, \end{cases} \quad (4.18)$$

and

$$v'_z(j) \equiv \frac{v_z(j+1) - v_z(j)}{x_z(j+1) - x_z(j)}. \quad (4.19)$$

The curvature $\kappa_z(j)$ has been plotted against the RG step index j in right panel of Fig. 8. For $z = 1$, the first derivative $v_z(j)$ becomes unity, so the second derivative $v'_z(j)$ (and hence the curvature) vanishes, leading to a flat (Minkowski) space. For $z > 1$, the curvature becomes negative, while it is positive for $z < 0$. All the flows lead to an asymptotically flat space (i.e., the curvature vanishes) as $j \rightarrow \infty$.

The different signatures of the emergent curvatures can be attributed to the different ways in which the mass of the theory scales under the decimation procedure. For $z > 0$, the curvature defined in eq. (4.17) can be written in terms of the beta function:

$$\kappa_z(j) = \frac{[e^{\beta(j)} - 1]^{\frac{1}{2}} j^{-z}}{[e^{\beta(j)+\beta(j+1)} - 1]^{\frac{3}{2}}} \left[\frac{e^{\beta(j+2)} - 1}{1 - e^{-\beta(j+1)}} - \frac{e^{\beta(j+1)} - 1}{1 - e^{-\beta(j)}} \right]. \quad (4.20)$$

This equation relates directly a geometric quantity (i.e., the curvature) of the bulk emergent space with the RG beta function for the field theory on the boundary. From Fig. 7, as the beta functions

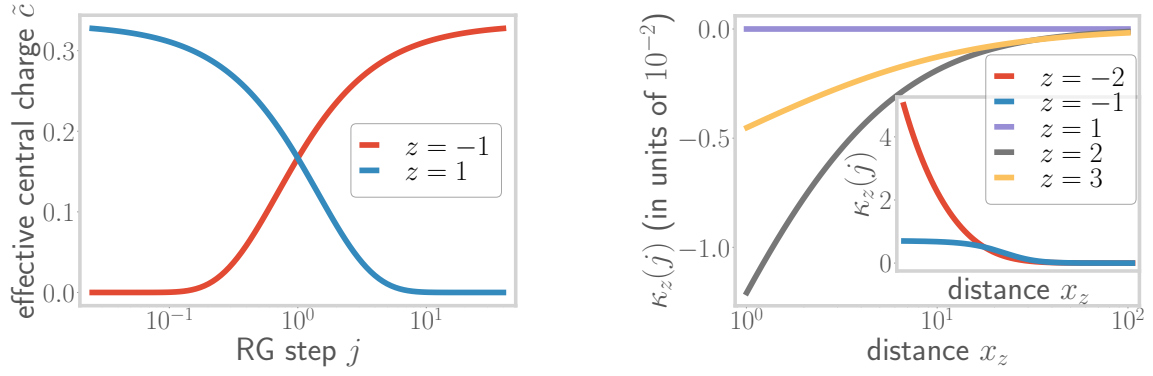


Figure 8. *Left:* Variation of the c -function under the RG transformations for relevant ($z = 1$, blue curve) and irrelevant ($z = -1$, red curve) RG flows. The end points are the fermionic central charge $c = 1/3$ and the off-critical massive value of 0. *Right:* Scaling of the curvature along the RG for multiple values of z . $z = 1$ leads to a flat spacetime with zero curvature, while $z > 1$ and $z < 1$ (inset) lead to negative and positive curvature respectively.

flow towards zero, we see from eq. (4.20) that the first fraction inside the square brackets is the first to vanish, followed by the second fraction. The sequential vanishing of these two fractions prior to the vanishing of the denominator $e^{\beta(j)} - 1$ in eq.(4.20) leads to the asymptotic vanishing of the curvature towards the fixed point. Different choices of $z > 0$ can be thought to represent different relevant perturbations that drive the system towards *gapped fixed points*, leading to distinct curvatures of the bulk. By employing the relation $v_z(j) = \Delta S_{j+1,z} / \Delta S_{j,z}$, eq. (4.17) can also be cast in terms of the entanglement entropy $S_{j,z}$, $S_{j+1,z}$ and $S_{j+2,z}$. The resulting non-linear relationship between $\kappa_z(j)$ and $S_{j,z}$ obtained is, however, in contrast to the linear dependence obtained by Cao et al. [220] between entanglement perturbations on the Hilbert space and the curvature of the resultant holographic space.

4.4 Topological nature of curvature sign

We will now argue that the signature of the curvature κ corresponds to a topological quantum number, and that a change in the signature as z is tuned through 1 amounts to a topological translation. For this, we first point out (following eq. 4.17) that the sign of the curvature is determined purely by the sign of $\gamma_z(j) \equiv 1 - v_z(j+1)/v_z(j)$ and $\alpha_z(j) = y_z(j+1) - y_z(j)$:

$$\kappa_z(j) = \frac{v'_z(j)}{[1 + v_z(j)^2]^{\frac{3}{2}}} = -\frac{\alpha_z(j) \gamma_z(j)}{(\Delta x_z(j))^2 [1 + v_z(j)^2]^{\frac{3}{2}}} \implies \text{sign}[\kappa_z(j)] = -\text{sign}[\alpha_z(j)] \text{sign}[\gamma_z(j)] . \quad (4.21)$$

We now promote j to a continuous complex variable with the real part being greater than or equal to 1: $\text{Re}[j] \geq 1$. The quantities $\alpha_z(j)$ and $\gamma_z(j)$ can be written as

$$\alpha_z(j) = \begin{cases} [(j+2)^z - (j+1)^z] \log 2, & z > 0 \\ [j^z - (j-1)^z] \log 2, & z < 0 \end{cases}, \quad \gamma_z(j) = \begin{cases} 1 - \frac{[(j+3)^z - (j+2)^z][(j+1)^z - j^z]}{[(j+2)^z - (j+1)^z]^2}, & z > 0 \\ 1 - \frac{[(j+1)^z - j^z]^2}{[j^z - (j-1)^z][(j+2)^z - (j+1)^z]}, & z < 0 . \end{cases} \quad (4.22)$$

As shown in Fig.9(left panel), the function γ_z is positive and monotonically decreasing for $z > 1$ or $z \leq -1$, and vanishes identically for $z = 1$. On the other hand, $\alpha_z(j)$ is positive for $z > 1$, zero at $z = 1$ and negative for $z \leq -1$ (see Fig.9(right panel)). Combining this, we find that the sign of

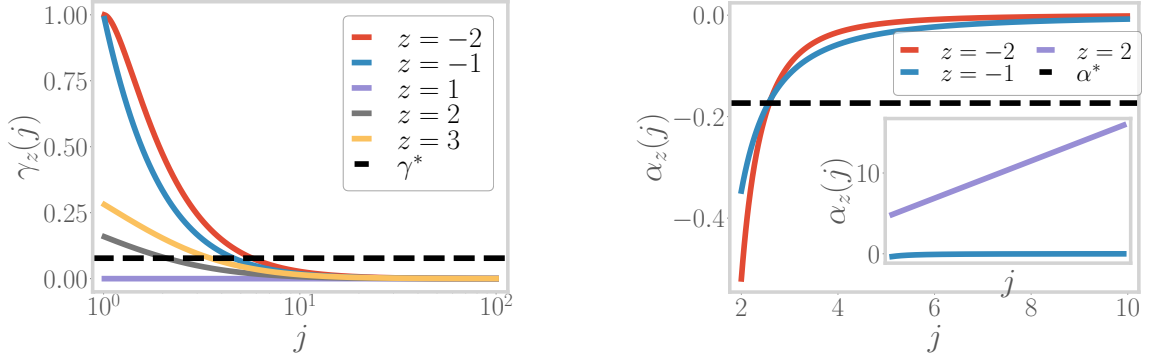


Figure 9. *Left:* Variation of γ_z along the RG for multiple values of $z > 0$. All trajectories for $z > 1$ intersect the line $y = \gamma^*$. *Right:* Variation of α_z along the RG for multiple values of $z < 0$. All trajectories intersect the line $y = \alpha^*$

the curvature can be written as:

$$\text{sign}[\kappa_z] = \begin{cases} -1, & z \geq 1 \\ 1, & z \leq -1 \end{cases} = \begin{cases} -\text{sign}[\gamma_z(j)], & z \geq 1 \\ -\text{sign}[\alpha_z(j)], & z \leq -1 \end{cases}. \quad (4.23)$$

We start by considering the region $z \geq 1$. Since $z = 0$ is excluded by definition, the denominator is always non-zero. This indicates that $\gamma_z(j)$ is continuous and monotonically decreasing in this range: the maximum value of $\{\gamma_z(j), j \in [1, \infty]\}$ occurs at $j = 1$. Further, the maximum value $\gamma_z(1)$ increases with the value of z , ranging between $\gamma_2(2)$ at $z = 2$ and unity at $z \rightarrow \infty$. These two features are demonstrated in the left panel of Fig. 9, and imply that all curves $\{\gamma_z(j) : j\}$ will take values both greater than and less than the value $\gamma^* \equiv \gamma_2(2)$ (dotted line in left panel of Fig. 9). Thus, the plot shows that there always exists a real value j_z^* for any given integer value $z > 1$ such that $\gamma_z(j_z^*) = \gamma^* = \gamma_2(2)$. This is precisely what ceases to happen for $z = 1$, as that is the only curve in the left panel of Fig. 9 that does not pass through γ^* .

Indeed, the difference between the curvature for the $z = 1$ and $z > 1$ classes can be captured by expressing the presence of the solution j_z^* in the form of a winding number. For this, we use the fact that the sign of $\gamma_j(z)$ is given by the following integral:

$$\text{sign}[\gamma_z(j)] \Big|_{z \geq 1} = \frac{1}{2\pi i} \oint_{\mathcal{C}} dj \frac{\partial}{\partial j} \ln[\gamma_z(j) - \gamma^*], \quad (4.24)$$

where the contour \mathcal{C} extends from $j = 1$ to $j = \infty$, and is shown in the left panel of Fig. 11. As the value of z is tuned from 2 to 1, the pole at j_z^* disappears and the integral reduces to zero. As shown in Fig. 10, the integral can thus be expressed as the winding number of the curve $\gamma_z(\mathcal{C}(j))$ that counts the number of times the contour $\gamma_z(\mathcal{C})$ winds around the singularity at γ^* :

$$\text{sign}[\gamma_z(j)] = \frac{1}{2\pi i} \oint_{\mathcal{C}} dj \frac{\partial(\gamma_z(j) - \gamma^*)}{\gamma_z(j) - \gamma^*} = \frac{1}{2\pi i} \oint_{\gamma_z(\mathcal{C})} \frac{d\gamma_z}{\gamma_z - \gamma^*}. \quad (4.25)$$

This is easily seen from the following argument. If we write a general complex variable y in the form $y = r e^{i\theta}$ and consider a general contour \mathcal{C} that starts from $r = r_0, \theta = 0$ and ends at $r = r_0, \theta = 2w\pi$ (such that the winding number of the curve is w), integrals of the form given above simplify and return the winding number itself:

$$\frac{1}{2\pi i} \oint_{\mathcal{C}} \frac{dy}{y} = \frac{1}{2\pi i} \int_{r_0}^{r_0} \frac{dr}{r} + \frac{1}{2\pi} \int_0^{2w\pi} d\theta = w, \quad (4.26)$$

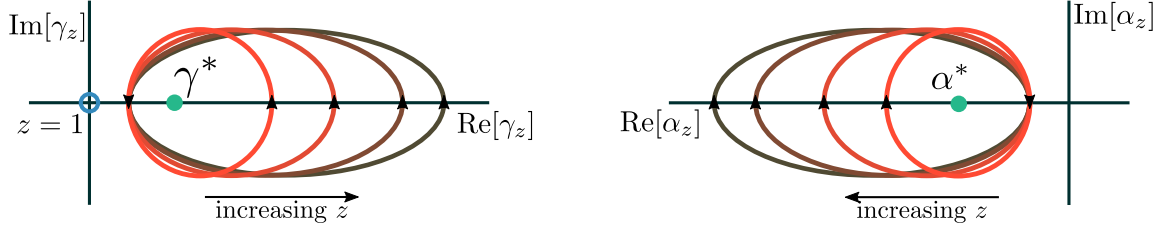


Figure 10. *Left:* Contours $\gamma_z(\mathcal{C})$ for multiple values of $z > 0$. As z increases, the contours extend in the positive $\text{Re}[\gamma_z]$ direction. *Right:* Contours $\alpha_z(\mathcal{C})$ for multiple values of $z > 0$. As z increases, the contours extend in the negative $\text{Re}[\gamma_z]$ direction.

where we used $dy = y \left(\frac{dr}{r} + d\theta \right)$.

The winding numbers take integer values, and are topological in nature: they are robust against geometric deformations, and change only when the curve crosses the singularity at $\gamma = \gamma^*$. Thus, for $z > 1$, the contour $\gamma_z(\mathcal{C})$ encloses the singularity at γ^* exactly once, leading to a winding number of unity. As z is lowered towards $z = 2$, the contours become smaller such that, in order to go from $z = 2$ to $z = 1$, the contour has to be moved across the singularity. This constituting a change in the topology of the contour: for $z = 1$, the contour no longer encloses the pole and the winding number is zero. In fact, at $z = 1$, the contour itself (depicted in blue) is of vanishing radius because $\gamma_1(j)$ has a constant value of zero. To complete the connection, we use eq. 4.21 to relate this topological winding number to the sign of the curvature:

$$\text{sign}[\kappa_z] \Big|_{z \geq 1} = -\mathcal{W}_z(\gamma^*), \quad (4.27)$$

where $\mathcal{W}_z(\gamma^*)$ is the winding number for $\gamma_z(\mathcal{C})$ around γ^* .

One can make a very similar argument for the case of $z \leq -1$. Here, as shown in the right panel of Fig. 3.10, the relevant quantity is $\alpha_z(j)$. For each curve α_z , the minimum value is at $j = 1$. For all z , this minimum starting value is largest for $z = -1$, and all subsequent curves $\alpha_z(j)$ start from even lower values. If we define a value $\alpha^* \equiv \alpha_z(j = 1)/2$, it is then clear that all curves $\alpha_z(j)$ will pass through the value α^* (dotted line in right panel of Fig. 3.10) at some value of j . This is very similar to the situation discussed just above for the case of $z \geq 1$ (with γ^* playing the role of α^*); we, therefore, employ the same technique here. Taking the same contour \mathcal{C} as defined above, we write the sign of α_z as the winding number of the curve $\alpha_z(\mathcal{C})$ around the point $\alpha_z = \alpha^*$

$$\text{sign}[\alpha_z(j)] \Big|_{z \leq -1} = -\mathcal{W}'_z(\alpha^*) = \frac{1}{2\pi i} \oint_{\alpha_z(\mathcal{C})} \frac{d\alpha_z}{\alpha_z - \alpha^*}. \quad (4.28)$$

For $z > 0$, α_z is positive, and the curve $\alpha_z(\mathcal{C})$ encloses points in the positive half of the real axis such that the winding number in the right panel of Fig. 10 is then zero. This indicates that the function $1 - 2\mathcal{W}'_z(\alpha^*)$ is unity for $z > 0$, leaving any other function in product with it unchanged. On the other hand, it is -1 for $z < 0$, returning the correct sign of $\alpha_z(j)$ in that range. Combining with eq. 4.27, the sign in the entire range can be expressed as

$$\text{sign}[\kappa_z] = \mathcal{W}_z(\gamma^*) \times [2\mathcal{W}'_z(\alpha^*) - 1]. \quad (4.29)$$

We can now summarise the topological nature of the sign of the curvature. For $z > 0$, the second winding number \mathcal{W}' is 0. As z varies from 2 to 1, the other winding number \mathcal{W} changes from 1 to 0, constituting the first topological change. In contrast, upon varying z from 1 to -1 , both winding numbers change: \mathcal{W} from 0 to 1, and \mathcal{W}' from 0 to 1. This constitutes the second topological change. Together, the two changes show that going from an open geometry (negative curvature) to a closed geometry (positive curvature) involves two topological transformations.

But what does this change in topology in the bulk mean for the boundary theory? As we now

discuss, this is brought about by the changes in the boundary conditions of the emergent space. As mentioned previously under eq. 4.3, the quantity z corresponds to the anomalous dimension of the spectral gap g_z in the effective field theory: a change in the sign of z corresponds to a change in the nature of the RG flow from relevance to irrelevance and vice-versa. The holographic nature of the RG flow dictates that such a change arises by a variation in some quantity in the parent interacting theory from which the effective field theory of non-interacting Dirac fermions can be thought to have originated. Indeed, such a change in the RG relevance has drastic consequences: a relevant spectral distance g_z implies a gap in the excitations at the fixed point, while an irrelevant g_z indicates the presence of gapless excitations. It can in fact be shown that the presence or absence of a gap in the effective theory at the fixed point determines the topology of the Fermi surface [106, 107]. In this way, the sign of the curvature is linked to the topology of the Fermi surface of the underlying interacting theory for the constituent fermions. Further, a change in the sign of the curvature corresponds to a topological transition of Fermi surface.

4.5 Embedding the emergent dimension on a metric space

We have shown above that the renormalisation group flow of the Hamiltonian leads to the emergence of an additional direction, quantified by the parameter x_j . The RG flow can be represented as an “information graph” $G(V, E)$, where the systems \mathcal{B}_j^1 (defined above eq. (4.9)) constitute the set of vertices $V = \{V_j\}$ and the mutual information $I_z^2(j : j')$ between the systems \mathcal{B}_j^1 and $\mathcal{B}_{j'}^1$, constitute the edges E_{ij} between the vertices. This information graph is characterised by an adjacency matrix whose elements are defined by the mutual information edge weights $I_z^2(j : j')$ [221]. This graph structure is shown in Fig. (6), with the red spheres indicating the vertices. In order to define a metric space, we will map the graph G to another graph \mathcal{G} that has the same vertices as G , but whose edges are weighted according to a well-defined notion of distance.

A path \mathcal{P} in \mathcal{G} is defined as a sequence of m vertices: $\mathcal{P}(V_1, V_2, \dots, V_m)$. The distance along the path is defined as the sum of distances along every pair of consecutive vertices: $l(\mathcal{P}) = \sum_{i=1}^{m-1} d(V_i, V_{i+1})$, where $d(V_i, V_{i+1}) = d(i, i+1)$ (see eq. (4.7)). The *geodesic* between two points V_i and V_j is the path \mathcal{P} which minimises the distance $l(\mathcal{P})$, and the distance along the geodesic then defines the *metric* $\tilde{d}(V_i, V_j)$ between two vertices V_i and V_j [220, 221]:

$$\tilde{d}(V_i, V_j) = \min_{\mathcal{P}} \{l(\mathcal{P})\} = \min_{\mathcal{P}} \left\{ \sum_{i=1}^{m-1} d(V_i, V_{i+1}) \right\}, \quad (4.30)$$

where the minimisation is carried out over all possible connected paths $\{\mathcal{P}\}$ between V_i and V_j , and m is the total number of vertices in a particular connected path \mathcal{P}_m . Following the expression for the distance $d(i, j)$ obtained in eq. 4.8, the metric takes the form

$$\tilde{d}(V_i, V_j) = \theta(z)j^z \ln 2 + \theta(-z)i^z \ln 2, \quad (i < j), \quad (4.31)$$

where we have assumed $i < j$, without loss of generality.

Finally, the metric dimension of the emergent space can be determined by finding the set with the lowest possible cardinality that can resolve the metric space [220, 222]. In order for a set to resolve the metric space, we must have $d(i, a) = d(j, a) \implies i = j$ for all points a in the set and for any pair of points i and j in the metric space. In our case, the singleton set $\mathcal{R} = \{0\}$ can resolve the metric space for $z > 0$, as $d(i, 0) = d(j, 0) \implies i^z = j^z \implies i = j$. Similarly, the singleton set $\mathcal{R} = \{\infty\}$ resolves the metric space for $z < 0$. As a result, we conclude that our emergent metric space is one-dimensional in nature.

4.6 Kinematics of the RG flows

Broader statements on the RG flow and the emergent holographic dimension can be made by studying quantities that can serve as candidates for the convergence parameter θ for the RG flows of g_z [223, 224]. We consider the following function as a candidate for the convergence parameter

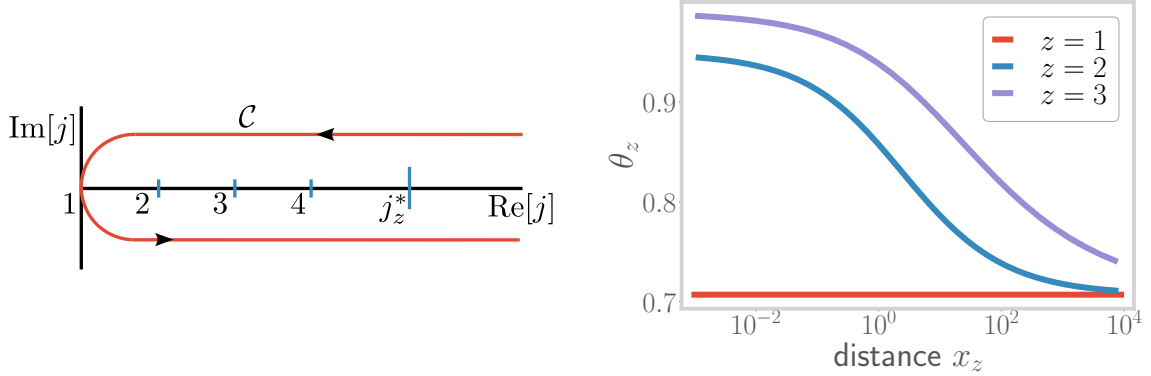


Figure 11. *Left:* The contour \mathcal{C} used in eq. 4.24 to calculate the winding number, corresponding to a loop that extends across all values of j . *Right:* Evolution of expansion parameter θ_z with distance x_z , leading to the fixed point at $\theta_z^* = 1/\sqrt{2}$.

for the case of $z > 0$:

$$\theta_z(j) = \frac{1}{\sqrt{v_z^{-2} + 1}} = \left[1 + \left\{ \frac{1 - e^{-\beta_z(j)}}{e^{\beta_z(j+1)-1}} \right\}^2 \right]^{-\frac{1}{2}}. \quad (4.32)$$

The parameter θ_z has been plotted in Fig. 11, and the behaviour is observed to be very similar to that of the beta function shown in Fig. 7. Indeed, this similarity describes the holographic nature of the RG flow: the emergent geometry (as seen through θ_z) is dictated by the RG flow described by β .

The quantity θ can be interpreted as an estimate of the rate of change of area enclosed by a fixed number of RG trajectories. To see that this is the case, we note that by using $v_j = \Delta y / \Delta x$, the expansion parameter can be written as $\theta = \Delta y(j) / \sqrt{\Delta x^2 + \Delta y^2} \sim \Delta g(j+1) / \sqrt{\Delta x^2 + \Delta y^2}$. Considering RG flows for $g_z(j)$ corresponding to multiple z , the area enclosed by the curves is given by the maximum g_z , and Δg_z is then the change in the area under the RG transformation. The denominator $\sqrt{\Delta x^2 + \Delta y^2}$ is the distance covered in the emergent spacetime, rendering θ as the rate of change of the area.

The equation of motion for this expansion parameter can then be obtained as:

$$\frac{d\theta_z}{dx} = \frac{v_z^{-3}}{(1 + v_z^{-2})^{\frac{3}{2}}} \frac{dv_z}{dx_j} = \kappa_z. \quad (4.33)$$

The simple form of this relation makes it clear that for relevant flows (corresponding to a negative curvature $\kappa_z < 0$), θ_z flows to a minimum. Following Fig. 8, this is accompanied by the minimisation of the c -function to zero. It is, therefore, tempting to conclude that eq. 4.33 for the spatial evolution of the convergence parameter θ is dual to eq. 4.16 that controls the flow of the c -function of the quantum theory along the RG flow.

4.7 Extension to the massive case

We will now generalise several of the main results obtained above to the case of two-dimensional electrons with a single-particle mass-gap $M_{n,\phi} = \sqrt{m^2 + \frac{4\pi^2}{L_x^2}(n+\phi)^2}$. Given that they depend only on the geometric part of the entanglement (which remains unchanged on introducing the mass $M_{n,\phi}$), the following set of key qualitative results and observations discussed earlier continue to hold for the case of a dispersion with a mass-gap:

- the hierarchical structure of the entanglement content (e.g., the area-law term in eqns.(3.14) and (3.17)) and the fact that the entanglement satisfies the Ryu-Takayanagi bound (right

panel of Fig.5),

- the dependence of the emergent distances x and y on the RG flow (Fig.6, eqns.(4.8) and (4.9)), and the fact that the RG beta function tracks the central charge (Fig.8),
- various qualitative and quantitative properties of the curvature (e.g., eq.(4.17)), including the topological nature of its sign (eq.(4.29)), and
- the existence of a convergence parameter that is related to the RG flow, and the equation that governs the evolution of the convergence parameter (eq.(4.33)).

The functional forms of certain other results do, however, undergo changes. For instance, the coupling $g_z(j)$ is given by the (more general) expression

$$g_z(n, j) = \ln \frac{M_{n+1, \phi}(j) - M_{n, \phi}(j)}{2\pi/L_x} = \ln \left[\sqrt{\tilde{m}^2 + (t_z(j)(n+1) + \phi)^2} - \sqrt{\tilde{m}^2 + (t_z(j)n + \phi)^2} \right], \quad (4.34)$$

where $\tilde{m} = mL_x/2\pi$ is a dimensionless parameter. We will work with the coupling for the mode $n = 0$:

$$g_z(0, j) = \ln \left[\sqrt{\tilde{m}^2 + (t_z(j) + \phi)^2} - \sqrt{\tilde{m}^2 + \phi^2} \right]. \quad (4.35)$$

In order to simplify the analysis, we work in the large mass limit $\frac{t_z + \phi}{\tilde{m}} \rightarrow 0$. In this limit, upon expanding the square root and retaining only the lowest order term, we obtain

$$g_z(0, j) = \ln \frac{[t_z(j) + \phi]^2 - \phi^2}{2\tilde{m}}. \quad (4.36)$$

The RG beta function $\beta = \ln(g_z(j+1)/g_z(j))$ can, in the large mass limit, then be related to the emergent distances x and y in terms of the coupling $g_z(j)$:

$$x_z(j) = \ln t_z(j) = \ln \left[\sqrt{2\tilde{m} e^{g_z(0, j)} + \phi^2} - \phi \right], \quad y_z(j) = \begin{cases} \ln \left[\sqrt{2\tilde{m} e^{g_z(0, j+1)} + \phi^2} - \phi \right], & z > 0, \\ \ln \left[\sqrt{2\tilde{m} e^{g_z(0, j-1)} + \phi^2} - \phi \right], & z < 0. \end{cases} \quad (4.37)$$

The quantitative dependence of the c -function on the RG beta function can also be expressed more generally as

$$e^{\beta_z(j)} = \left[\ln \frac{\left(\frac{\tilde{c}(j+1)}{c} + \phi \right)^2 - \phi^2}{2\tilde{m}} \right] \left[\ln \frac{\left(\frac{\tilde{c}(j)}{c} + \phi \right)^2 - \phi^2}{2\tilde{m}} \right]^{-1}. \quad (4.38)$$

Quantities such as the curvature κ and the convergence parameter θ can similarly be expressed in terms of the coupling $g_z(j)$.

5 Topological content of the entanglement spectrum

We focus on the massless case $m = 0$ in the remainder of this work. First, we will show how to obtain Luttinger's volume (eq.(2.8)) from the g -partite information entanglement measure I^g of a system of massless 2D electrons. By considering the entanglement spectrum of the same system in a transverse magnetic field, we will then extract the Chern number of the integer quantum Hall ground state.

5.1 Luttinger's volume for massless 2D electrons

The flux-dependent part of the g -partite information I^g can be used to probe the k -space volume V_L within the Fermi surface. We define a quantity $Q_g(\phi)$ that is periodic in the flux ϕ and independent of the geometry:

$$Q_g(\phi) = f_{g,z} \left[\frac{1}{\sqrt{2}} - \frac{1}{2} e^{-\frac{1}{c}} \left(I_{\{\mathcal{A}_{i,z}\}}^g(\phi) - I_{\{\mathcal{A}_{i,z}\}}^g(\phi^{(0)} f_{g,z}) \right) \right] = f_{g,z} \left[\frac{1}{\sqrt{2}} - |\sin(\pi \phi f_{g,z})| \right], \quad (5.1)$$

where $\phi^{(0)} = \frac{1}{6}$ is the value at which the flux-dependent part of $S_0(\phi)$ vanishes. Further, from eq.(3.19), we have

$$I_{\{\mathcal{A}_{i,z}\}}^g(\phi_g) - I_{\{\mathcal{A}_{i,z}\}}^g(\phi_g^{(0)} f_{g,z}) = -c \ln(2 |\sin(\pi \phi f_{g,z})|). \quad (5.2)$$

Note that the non-differentiability of $Q_g(\phi)$ at $\phi f_{g,z} = 0, 1, 2, \dots$ is not a concern as ϕ is chosen to be non-integral, ensuring that $\phi f_{g,z}$ is also non-integral.

In order to express the number N_L^x of positive k_x -states available inside the Fermi surface in the x -direction in terms of $Q_g(\phi)$, we need to establish a relation between the flux ϕ and the Fermi surface. The k_x -states of interest to us are given by $k_x^n = \frac{2\pi n}{L_x}$, $n \in \mathbb{Z}$, $0 \leq k_x^n \leq k_x^F$, where k_x^F is the x -component of the Fermi momentum \vec{k}_F . Assuming the flux-free Hamiltonian has time-reversal symmetry, there should be an equal number of states with the opposite momenta. Let n^* be the integer for which $k_x^{n^*} \leq k_x^F$ and $k_x^{n^*+1} > k_x^F$. Since the flux couples to the k_x -states as $k_x^n \rightarrow k_x^n + eA = \frac{2\pi n + 2\pi \phi}{L_x}$, tuning ϕ by 1 leads to the entire spectrum of k_x -states being shifted by one quantum number: $k_x^n \rightarrow \frac{2\pi(n+1)}{L_x} = k_x^{n+1}$. This means that the state $k_x^{n^*}$ moves to $k_x^{n^*+1}$, and hence out of the Fermi volume by crossing k_x^F . This flow of the spectrum is shown in Fig. 14.

If we now connect the system to a particle reservoir with the chemical potential set to zero, any k_x -state that moves out of the Fermi volume becomes unoccupied. We continue tuning the flux to a value ϕ^* , where the system becomes entirely devoid of any particles. The number of k_x -states that are below k_x^F can then be said to be given by the number of times ϕ goes through an integer value while changing from 0^+ to $\phi^* + 0^+$. Since we do not set the flux to an integer value, we can equivalently count the number of times ϕ goes through, say, three-quarters of an integer - $j - \frac{1}{4} : j = 1, 2, \dots$ - in changing from 0^+ to $\phi^* - 0^+$. We will now show that this count can be expressed in terms of Q_g . We begin by considering $Q_0(\phi) = \frac{1}{\sqrt{2}} - |\sin \pi \phi|$. At every three-quarter value of the flux, the quantity $\phi_j = j - \frac{1}{4} : j = 1, 2, \dots$, $|\sin \pi \phi_j|$ attains the value of $\sin \frac{\pi}{4} = \frac{1}{\sqrt{2}}$, such that $Q_0^{-1}(\phi)$ goes through a simple pole. Each such pole ϕ_j can be picked up via a complex integral around a contour \mathcal{C}_j that encloses the pole:

$$-f_j \frac{1}{2\sqrt{2}i} \oint_{\mathcal{C}_j} \frac{d\phi}{Q_0(\phi)} = 1, \quad (5.3)$$

where f_j is either +1 or -1 and is defined through the equation $|\sin(\pi(j - \frac{1}{4}))| = f_j \sin(\pi(j - \frac{1}{4}))$, and \mathcal{C}_j is a circle of diameter 1/4 centered at $\phi = j - \frac{1}{4}$ (shown in Fig. 12). The evaluation of the integral eq.(5.3) is shown in Appendix C. In order to drop the sign prefactor f_j , we reorient those contours for which f_j is +1, and such that they wind around in the clockwise direction. The contours are shown in the left panel of Fig. 13, and defined as

$$\mathcal{C}_j(\phi) = \left\{ \phi : \phi = j - \frac{1}{4} + \frac{1}{8} e^{i\theta}, \theta \in [0, -2\pi f_j] \right\}, \quad (5.4)$$

such that they host a singularity at their center. With this redefinition of the contours, we have

$$\frac{1}{2\sqrt{2}i} \oint_{\mathcal{C}_j} \frac{d\phi}{Q_0(\phi)} = 1. \quad (5.5)$$

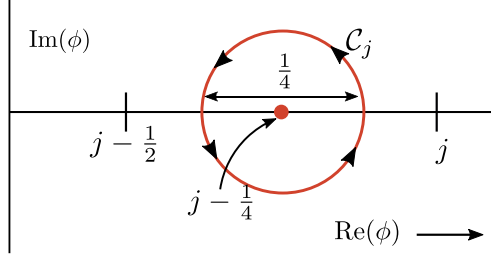


Figure 12. Contour \mathcal{C}_j used to integrate eq. 5.3, with its center at $j - \frac{1}{4}$ and diameter being $\frac{1}{4}$.

Counting the number of three-quarter values then reduces to counting the number of poles of Q_0^{-1} in the above-mentioned range $\phi \in (0, \phi^*)$. In this way, we can now express the count N_L^x in terms of Q_0 :

$$N_L^x = \frac{1}{2} \sum_{j=1}^{\phi^*} \frac{1}{2\sqrt{2}i} \oint_{\mathcal{C}_j(\phi)} \frac{d\phi}{Q_0(\phi)} = \frac{1}{2\sqrt{2}} \sum_{j=1}^{\phi^*} \frac{1}{2i} \oint_{\mathcal{C}_j(\phi)} \frac{d\phi}{Q_0(\phi)}. \quad (5.6)$$

The factor of half in eq.(5.6) is required as we want to count only the number of positive momentum states (and which is equal to the number of negative momentum states).

In going from $Q_0(\phi)$ to a general $Q_g(\phi)$, the only change required is to redefine $\phi \rightarrow \phi_g = f_{g,z}\phi$. This implies that while the states in k -space have become more coarse-grained, the flux ϕ has become more fine-tuned by the same scaling factor. This is a reflection of the overall conservation of particle number density: keeping the chemical potential fixed, the increased spacing between the k_x -states implies that a smaller number of particles are now occupying an equally smaller volume. As the number density is conserved, so is the Luttinger volume (eq.(2.8)). Thus, given that $\phi_g^* = \phi^*$, the expression for N_L^x remains practically unchanged:

$$N_L^x = \frac{1}{2\sqrt{2}} \sum_{j=1}^{\phi^*} \frac{1}{2i} \oint_{\mathcal{C}_j(\phi_g)} \frac{d\phi_g}{\frac{1}{\sqrt{2}} - |\sin \pi \phi_g|}. \quad (5.7)$$

In order to rewrite N_L^x in terms of the flux ϕ , we start by making the substitution $\phi_g \rightarrow f_{g,z}\phi$:

$$N_L^x = \frac{1}{2\sqrt{2}} \sum_{j=1}^{\phi^*} \frac{1}{2i} \oint_{\mathcal{C}_j(f_{g,z}\phi)} \frac{f_{g,z}d\phi}{\frac{1}{\sqrt{2}} - |\sin(\pi f_{g,z}\phi)|}. \quad (5.8)$$

In the above equation, we can recognise $\frac{f_{g,z}}{\frac{1}{\sqrt{2}} - |\sin(\pi f_{g,z}\phi)|}$ as $Q_g^{-1}(\phi)$. Also note that the contour can be written as

$$\mathcal{C}_j(f_{g,z}\phi) \equiv \mathcal{C}_j^g(\phi) = \left\{ \phi : \phi = t_{g,z} \left(j - \frac{1}{4} + \frac{e^{i\theta}}{8} \right), \theta \in [0, -2\pi f_j] \right\}. \quad (5.9)$$

These curves are again circles of radius $1/8$, but centered at $t_{g,z} \times (1 - \frac{1}{4})$, $t_{g,z} \times (2 - \frac{1}{4})$, $t_{g,z} \times (3 - \frac{1}{4})$ and so on. These are simply a generalisation of the curves defined in Eq. 5.4; the curves for $t_{g,z} = 2$ are shown in the right panel of Fig. 13. Substituting this in eq.(5.8) gives

$$N_L^x = \frac{1}{2\sqrt{2}} \sum_{j=1}^{\phi^*} \frac{1}{2i} \oint_{\mathcal{C}_j^g(\phi)} \frac{d\phi}{Q_g}. \quad (5.10)$$

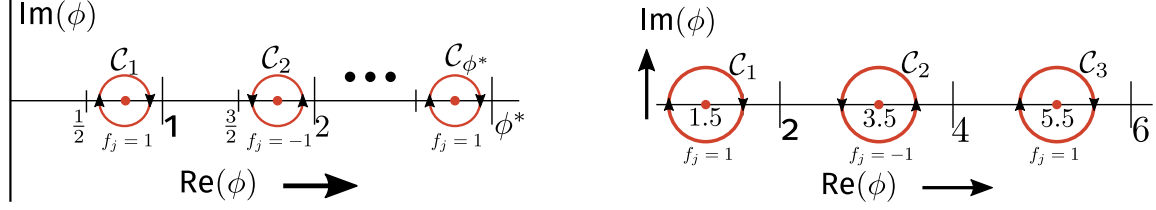


Figure 13. *Left:* Contours \mathcal{C}_j used to integrate over Q_0^{-1} in eq. 5.6. Dotted vertical lines represent integer values of $\text{Re}(\phi)$. All contours start and end within two adjacent integer values. The final contour \mathcal{C}_{ϕ^*} ends just short of $\text{Re}(\phi) = \phi^*$. Note the alternating direction of the contours brought about by the alternation of f_j in going from $j = 1$ to $j = 2$, and so on. *Right:* Contours \mathcal{C}_j^g for $t_{g,z} = 2$, centered at $2(1 - \frac{1}{4})$, $2(2 - \frac{1}{4})$ and $2(3 - \frac{1}{4})$. Note the alternating directions of the contours.

For a spatially isotropic system, the Fermi volume is given by

$$V_L = v_2 \times \pi (N_L^x)^2 = \frac{1}{2} \frac{\pi^3}{V} \left[\sum_{j=1}^{\phi^*} \frac{1}{2i} \oint_{\mathcal{C}_j^g(\phi)} \frac{d\phi}{Q_g(\phi)} \right]^2, \quad (5.11)$$

where V is the real space volume of the system, and $v_d = (2\pi)^d / V$ is the volume of the smallest unit in k -space. For a generally anisotropic Fermi volume, each direction in the d -dimensional k -space can be completely specified by an angular coordinate θ with respect to some predefined coordinate system. For each direction $\hat{\theta}$, we can insert a gauge field $\vec{A} = A\hat{\theta}$ and take the thin torus limit in this direction, obtaining thereby the g -partite information $I^g(\phi_\theta)$ for length l in the direction perpendicular to $\hat{\theta}$. With the θ -dependent I^g , one can then define the quantity $Q_g(\phi_\theta)$ which counts the number of states N_L^θ in the direction $\hat{\theta}$ inside the Fermi volume. In this way, the total Fermi volume can be obtained by integrating over θ :

$$V_L = \frac{\pi^2}{4V} \int_0^{2\pi} d\theta \left[\sum_{j=1}^{\phi_\theta^*} \frac{1}{2\pi i} \oint_{\mathcal{C}_j^g(\phi)} \frac{d\phi}{Q_g(\phi)} \right]^2. \quad (5.12)$$

It is important to note that the quantity V_L is independent of the RG index g , and is thus identical in value for all g members of the hierarchy at the g th step of the coarse-graining process.

The topological nature of Luttinger volume can be made further manifest by expressing it in terms of winding numbers, following Ref.[104] for the case of interacting electrons. To do so, we point out that the integrand $Q_g^{-1}(\phi)$ can be written as a derivative:

$$\frac{1}{Q_g(\phi)} = \frac{\sqrt{2}}{\pi} \frac{\partial}{\partial \phi} \ln Y_j^g = \frac{\sqrt{2}}{\pi} \frac{1}{Y_j^g} \frac{\partial Y_j^g}{\partial \phi}, \quad (5.13)$$

where

$$Y_j^g(\phi) \equiv \left[\frac{f_j \tan 3\pi/8 - \tan(\pi f_{g,z} \phi/2)}{\tan(\pi f_{g,z} \phi/2) - \tan(\pi/8)} \right]^{f_j} = \begin{cases} \frac{\tan 3\pi/8 - \tan(\pi f_{g,z} \phi/2)}{\tan(\pi f_{g,z} \phi/2) - \tan(\pi/8)}, & \text{when } j = \text{odd, and} \\ \frac{\tan(\pi f_{g,z} \phi/2) + \tan(\pi/8)}{-\tan 3\pi/8 - \tan(\pi f_{g,z} \phi/2)}, & \text{when } j = \text{even.} \end{cases} \quad (5.14)$$

Substituting this into the expression for 2-dimensional isotropic Luttinger volume in eq. 5.11, we obtain

$$V_L = \frac{\pi^3}{V} \left[\sum_{j=1}^{\phi^*} \frac{1}{2\pi i} \oint_{\mathcal{C}_j^g} \frac{dY_j^g}{Y_j^g} \right]^2. \quad (5.15)$$

As before, the specific integral in the above expression is actually a winding number that counts

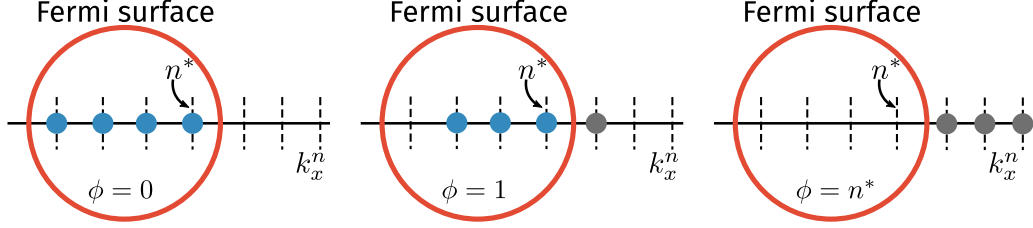


Figure 14. Spectral flow of the states within the Fermi volume. The red curve represents the Fermi surface. Upon tuning the flux ϕ , the k -space states (indicated in the form of dotted lines along the k_x -axis) are shifted towards the Fermi surface. The blue circles represent electrons with momenta below k_F , and are part of the ground state. On the other hand, the grey circles represent particles with momenta above k_F : they have moved out of the system, and into the reservoir connected to it (see discussion in main text). Each time ϕ changes by 1, the state nearest to the Fermi surface moves out of the Fermi volume. Tuning ϕ by n^* empties the entire Fermi volume.

the number of times the contour $Y_j^g(\mathcal{C}_j^g)$ winds around the singularity at $Y_j^g = 0$. Note that these are the same singularities that exist at the centers of the contours \mathcal{C}_j^g and that are picked up in, for example, eq. 5.3. To demonstrate this, we point out that the centers of the contours are given by $\phi = t_{g,z}(j - \frac{1}{4})$, $j = 1, 2, \dots, \phi^*$. At these values, we have

$$\tan\left(\frac{\pi f_{g,z}\phi}{2}\right) = \tan\left(\frac{\pi j}{2} - \frac{\pi}{8}\right) = \begin{cases} \tan\frac{3\pi}{8}, j = 1, 3, \dots \\ -\tan\frac{\pi}{8}, j = 2, 4, \dots \end{cases} \quad (5.16)$$

Comparing with eq. 5.14, we can see that the numerators of Y_j^g are zero at these values of ϕ for both even and odd values of j . This leads to $Y_j^g = 0$, and hence a singularity in $\frac{dY_j^g}{Y_j^g}$. These values of the flux are therefore the common singularities that are picked up by the poles of $Q_g^{-1}(\phi)$ as well as the winding numbers.

We now define w_j^g as the winding number for the curve $Y_j^g(\mathcal{C}_j^g)$ around $Y_j^g = 0$, and $\mathcal{W}(\phi^*) = \sum_{j=1}^{\phi^*} w_j^g$ as the total winding number for all the curves $\{Y_j^g(\mathcal{C}_j^g), j = 1, 2, \dots\}$. Then, the isotropic Fermi volume takes the compact form

$$V_L = \frac{\pi^3}{V} \mathcal{W}(\phi^*)^2. \quad (5.17)$$

5.2 Chern number of the integer quantum Hall state

Interestingly, the above method employed in using entanglement measures to extract the Luttinger volume can also be applied (with suitable modifications) to an integer quantum hall system (generated upon placing the system in a strong transverse magnetic field) to obtain the number of filled Landau levels (a Chern number). To begin, we imagine a system of free non-relativistic electrons in a cylinder geometry (fig. 15), and placed in a magnetic field $\nabla \times \vec{A} = \vec{B}$ that points radially outwards. The field \vec{B} generates Φ flux quanta through the surface of the cylinder. An Aharonov-Bohm flux $\vec{A}' = -2\pi\phi/L_x\hat{x}$ is also placed in the x -direction (i.e., along the circumference of the cylinder). We divide the cylinder into two subsystems A and B (fig. 15), such that tuning the dimensionless flux ϕ by 1 transfers a charge equal to the first Chern number, from A to B . The translation invariance in the x -direction ensures that the momentum k_x are good quantum numbers; for each value of k_x , we can define the matrix elements of the single-particle correlation matrix $G(k_y)$ for the subsystem A as [225, 226]

$$G_{ij}^A(k_x) = \langle \psi_{\text{gs}} | c_{k_x,i}^\dagger c_{k_x,j} | \psi_{\text{gs}} \rangle, \quad (5.18)$$

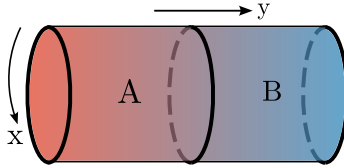


Figure 15. Cylindrical geometry for the integer quantum Hall system, with a magnetic field \vec{B} pointing radially outwards through the surface of the cylinder. An Aharonov-Bohm flux vector potential acts in the x -direction (i.e., along the circumference). The entanglement is calculated between the subsystem A and its complement B .

where $|\psi_{\text{gs}}\rangle$ is the ground state and i, j represent the degrees of freedom other than k_x . The total matrix G^A is constructed by joining the smaller blocks $G^A(k_x)$. As ϕ is varied, the variation of the trace of the flux-dependent matrix $G^A(\phi)$ is linear in the flux ϕ : $\text{Tr}[G^A(\phi)] - \text{Tr}[G^A(0)] = -\frac{1}{e}\sigma_H\phi$. This implies that as long as there are extended states at sufficiently small energies, we will have spectral flow that can be captured through the integral:

$$-\frac{\sigma_H}{2\pi i e} \int_{\mathcal{C}_H} \frac{d\phi}{\text{Tr}[G^A(\phi)] - \text{Tr}[G^A(0)]}, \quad (5.19)$$

where \mathcal{C}_H is a circle of radius $1/2$ in the complex plane centered at $\phi = 0$. This integral is zero if there is no spectral flow, i.e., the effect of the gauge field can be removed by a gauge transformation and the trace is insensitive to the flux. In order to count the number of filled Landau levels (essentially, the filling factor ν), we can now vary the flux quanta Φ (due to \vec{B}) so as to change the filling from ν to 0:

$$\nu = -\frac{\sigma_H}{2\pi i e} \sum_{\Phi'=\Phi}^{\Phi^{\text{max}}} \int_{\mathcal{C}_H} \frac{d\phi}{\text{Tr}[G_{\Phi'}^A(\phi)] - \text{Tr}[G_{\Phi'}^A(0)]}. \quad (5.20)$$

The subscript Φ' on G^A indicates that the correlations depend on the variable magnetic field \vec{B}' . The upper limit Φ^{max} is given by the lowest value of the magnetic field \vec{B}' for which only one Landau level is filled. The magnetic field is varied such that exactly an integer number of Landau levels are filled at any given value. Importantly, the filling factor ν is known to be a Chern number $\mathcal{C}(\Phi)$ [15, 227].

We can also relate eq. (5.20) to the entanglement of the system by introducing the entanglement spectrum [4, 17], which refers to the set of eigenvalues $\{\lambda_\chi^A(k_x)\}$ of the reduced density matrix $\rho^A(k_x)$ for subsystem A corresponding to the momentum mode k_x in the x -direction and χ is a particular configuration of the degrees of freedom $\{i\}$ in the y -direction. We have the relation [226]

$$\lambda_\chi^A(k_x) = \text{Det}[P_\chi G^A(k_x) (1 - P_\chi) G^A(k_x)], \quad (5.21)$$

where P_χ is an operator that projects on to the subset of states $\{j\}$ in $\{i\}$ that are occupied in the configuration χ . This relation between G^A and the eigenvalues λ then leads to the same conclusion as in the case without the magnetic field: the pole structure of the entanglement spectrum encodes the topological information of the system revealed in eq.(5.20). In the case of zero magnetic field, the topological quantity revealed from the pole structure was a winding number (\mathcal{W}), while in the present case it is a Chern number.

Finally, we reveal the connection between the winding numbers \mathcal{W} in the metallic case and the Chern numbers in the integer quantum Hall system. The degeneracy of each Landau level is equal to the number of flux quanta Φ' generated by the magnetic field B' . Since the total number of particles in the system is fixed, the electronic states of the filled Fermi sea that form the Luttinger volume (in the absence of the external B-field) are redistributed into the Landau levels with the appropriate degeneracy as a strong transverse magnetic field is turned on. Thus, we have the constraint that $\mathcal{C} \times \Phi'$ is a constant, where \mathcal{C} is the Chern number describing the quantum hall state

at flux Φ' and equal to the number of filled Landau levels. From eq. (5.17), this constraint helps relate \mathcal{C} to the winding number $\mathcal{W}(\phi^*)$:

$$\mathcal{C} \times \Phi' = \left\lfloor \frac{\pi}{4} \mathcal{W}(\phi^*)^2 \right\rfloor, \quad (5.22)$$

where $\lfloor \cdot \rfloor$ is the floor function and returns the largest integer less than or equal to the argument.

6 Conclusions and Outlook

In summary, we have shown that increasing or decreasing the spacing between adjacent modes in k -space of a system of non-interacting electrons in $2 + 1$ -dimensional theory leads to hierarchical arrangement of the entanglement with scale, and that the geometrical part of this renormalisation of the entanglement can be described as the emergence of an additional spatial dimension. Specifically, the mass induced by the dimensional reduction procedure of the $2 + 1$ -dimensional theory to one described by $1 + 1$ -dimensional modes enables the definition of a coupling g that quantifies the spectral gap, and the RG beta function β for g can be related to the distance in the emergent spatial dimension. Such a relation serves as a concrete demonstration of a holographic mapping between the bulk and boundary theories. We also define a curvature κ along the additional spatial dimension: κ can also be related to the beta function β and takes all three possible signs, obtaining flat as well as curved spaces with and without boundaries. We also prove that changing from flat to curved space involves a topological transition, which can be traced to a change in the topology of the Fermi surface of the boundary theory and the presence (or absence) of gapless excitations lying proximate to it. For the massless case $m = 0$, the presence of a boundary condition changing Aharonov-Bohm flux adds generates a geometry-independent term in the entanglement entropy: the topological nature of this term is displayed by relating it to the Luttinger volume of the gapless fermionic system. The Luttinger volume is also shown to be invariant under the coarse graining procedure. Finally, by placing the system of $2 + 1$ dimensional electrons in a perpendicular magnetic field, we argue that the Chern number topological invariant for the ground states of the integer quantum Hall ground system are constrained by the value of the Luttinger volume in the underlying metallic system (i.e., prior to the insertion of the field).

How robust are our conclusions towards the inclusion of electronic correlations? Given the adiabatic continuity that links Fermi liquids to the non-interacting Fermi gas, i.e., the preservation of the k -space quantum numbers under adiabatic inclusion of (screened) inter-particle interactions, we expect our results to be equally valid for the many-particle entanglement of the excitations described by the fixed point effective theory for the Fermi liquid. Non-Fermi liquids are, however, not adiabatically continuous to the Fermi gas. Thus, it should be interesting to adapt our approach to the study of interacting models of electrons that lead to gapless non-Fermi liquids (including those that are known to appear at quantum critical points related to the breakdown of a Fermi liquid). For instance, Ref.[228] reports that the second Renyi entropy of a thin k -space shell proximate to the Fermi surface is related to the quasiparticle residue; how would this change in a non-Fermi liquid? It also appears interesting to identify the effects of electronic correlations on various aspects of the emergent space. The renormalisation group techniques applied in Refs.[228–232] could also be worth investigating towards answering these questions.

It is interesting to note that our results point towards a broader similarity between the gapless fermionic systems considered here and gapped topologically ordered quantum liquids. Recall that the latter are known to possess a ground state degeneracy that is dependent on the topological nature of the interacting electronic system, leading to a subsystem entanglement entropy that has a geometry-independent subleading piece (S_{topo}) referred to as the topological entanglement entropy. It was shown by some of us recently [207] that for a collection of N subsystems (CSS) that form a closed annular structure, the n -partite quantum entanglement information measures I^n ($3 \leq n \leq N$) are a topological invariant equal to the product of S_{topo} and the Euler characteristic of the planar manifold on which the CSS is embedded. This appears to be analogous to our finding of the hierarchical sequence of quantities $\{Q_g\}$ defined at a particular RG step (and arising out of

the topological flux-dependent piece of the entanglement entropy), all of whom encode the same Luttinger volume for the gapless systems we have studied (eq.5.12). Further, the robustness of the n -partite information I^n against small deformations of the CSS in a topologically ordered system can be compared to the invariance of N_L^x to small deformations of the contours $\mathcal{C}_1, \mathcal{C}_2, \dots$ (see right panel of Fig. 13). It appears tempting to speculate on a possible universal origin underlying these similarities.

Our results lead to a number of interesting questions. Firstly, the convergence parameter θ is reminiscent of the expansion rate of congruence flows on Riemannian manifolds in the context of the Raychaudhuri equation [223]. While the evolution equation for θ (eq.4.33) obtained by us is not of the same form (as there is no time variable, neither is there a θ^2 term in the expansion rate), we do expect such an equation to hold for an appropriately defined expansion parameter [224, 233]. This likely requires the introduction of temporal dynamics of the emergent spatial dimension, and lies well beyond the purview of the present work. Secondly, it remains to be seen how the geometry-independent part of the entanglement behaves in the presence of a mass ($m > 0$) for the Dirac fermions: a spectral gap is expected to have consequences for Luttinger's theorem [106], as well as for the many-particle entanglement. For instance, Ref.[228] reports that the second Renyi entropy shows the signatures of the condensation of Cooper pairs in the BCS problem.

Finally, we would like to point out an interesting conclusion that emerges from our analysis. The large entanglement entropy for noninteracting fermions arises from the non-local nature of the Hamiltonian (and the associated ground state wavefunction) in real space. The hierarchy in the multipartite entanglement I^g found by us is equally striking, and indicates the presence of up to N -partite entanglement for a subsystem of N modes. This can also be seen by writing the entanglement (or modular) Hamiltonian $\mathbb{H} = -\ln \rho$, where ρ is the density matrix of the ground state. Such an entanglement Hamiltonian will have up to N -particle interaction terms arising from the non-zero multipartite information: $\mathbb{H} = \sum_i \epsilon_i^{(1)} \hat{n}_i + \sum_{i,j} \epsilon_{i,j}^{(2)} \hat{n}_i \hat{n}_j + \sum_{i,j,k} \epsilon_{i,j,k}^{(3)} \hat{n}_i \hat{n}_j \hat{n}_k + \dots$. The eigenvalues of this Hamiltonian (i.e., the modular energies) constitute the entanglement spectrum. Indeed, the entanglement Hamiltonian can be visualised as a hypergraph with the indices $\{i\}$ making up the nodes of the network and the coefficients $\epsilon_{i_1, i_2, \dots, i_n}^{(n)}$ are weighted hyperedges (a hyperdimensional edge connecting n nodes, where n can be greater than 2) connecting the nodes $\{i_1, i_2, \dots, i_n\}$. Considering only the two-particle coefficients $\epsilon^{(2)}$ (these are the terms that produce mutual information) leads to a graph with only simple edges (each edge connects only two nodes): we find that the RG evolution of this simple graph is related to the emergent spatial direction through the holographic principle. However, we are yet to see whether the higher dimensional edges (the part of the entanglement spectrum that lead to tripartite information, 4-partite information and so on) also have a holographic interpretation; further, what kind of spaces they may lead to. We note that studies of the time-variation of tripartite information during an equilibrium process after the injection of energy suggest that it remains negative throughout the process [234–236], indicating that care must be taken in defining geometric measures using it. Nevertheless, our study raises the possibility of obtaining a generalisation of the gauge-gravity duality from the perspective of many-particle entanglement.

Acknowledgments

AM thanks IISER Kolkata for funding through a junior and a senior research fellowship. SP thanks the CSIR, Govt. of India for funding through a senior research fellowship. SL thanks the SERB, Govt. of India for funding through MATRICS grant MTR/2021/000141 and Core Research Grant CRG/2021/000852. The authors thank N. Banerjee and S. G. Choudhury for fruitful discussions and feedback.

References

- [1] B.M. Terhal, M.M. Wolf and A.C. Doherty, *Quantum entanglement: A modern perspective*, *Physics Today* **56** (2003) 46 [<https://doi.org/10.1063/1.1580049>].

- [2] R. Horodecki, P. Horodecki, M. Horodecki and K. Horodecki, *Quantum entanglement*, *Reviews of modern physics* **81** (2009) 865.
- [3] J. Eisert, M. Cramer and M.B. Plenio, *Colloquium: Area laws for the entanglement entropy*, *Rev. Mod. Phys.* **82** (2010) 277.
- [4] N. Laflorencie, *Quantum entanglement in condensed matter systems*, *Physics Reports* **646** (2016) 1.
- [5] B. Zeng, X. Chen, D.L. Zhou and X.-G. Wen, *Quantum information meets quantum matter*, Springer (2019).
- [6] M. Erhard, M. Krenn and A. Zeilinger, *Advances in high-dimensional quantum entanglement*, *Nature Reviews Physics* **2** (2020) 365.
- [7] X.G. Wen, *Topological orders in rigid states*, *International Journal of Modern Physics B* **04** (1990) 239 [<https://doi.org/10.1142/S0217979290000139>].
- [8] X.G. Wen and Q. Niu, *Ground-state degeneracy of the fractional quantum hall states in the presence of a random potential and on high-genus riemann surfaces*, *Phys. Rev. B* **41** (1990) 9377.
- [9] X. Wen and A. Zee, *Quantum statistics and superconductivity in two spatial dimensions*, *Nuclear Physics B - Proceedings Supplements* **15** (1990) 135.
- [10] X.-G. Wen, *Topological orders and chern-simons theory in strongly correlated quantum liquid*, *International Journal of Modern Physics B* **05** (1991) 1641.
- [11] X.-G. Wen, *Topological orders and edge excitations in fractional quantum hall states*, *Advances in Physics* **44** (1995) 405.
- [12] X.-G. Wen, *Topological order: From long-range entangled quantum matter to a unified origin of light and electrons*, *ISRN Condensed Matter Physics* **2013** (2013) 198710.
- [13] X.-G. Wen, *Colloquium: Zoo of quantum-topological phases of matter*, *Reviews of Modern Physics* **89** (2017) 041004.
- [14] R. Tao and Y.-S. Wu, *Gauge invariance and fractional quantum hall effect*, *Phys. Rev. B* **30** (1984) 1097.
- [15] Q. Niu, D.J. Thouless and Y.-S. Wu, *Quantized hall conductance as a topological invariant*, *Physical Review B* **31** (1985) 3372.
- [16] X.G. Wen, *Vacuum degeneracy of chiral spin states in compactified space*, *Phys. Rev. B* **40** (1989) 7387.
- [17] H. Li and F.D.M. Haldane, *Entanglement spectrum as a generalization of entanglement entropy: Identification of topological order in non-abelian fractional quantum hall effect states*, *Physical review letters* **101** (2008) 010504.
- [18] X.-L. Qi, H. Katsura and A.W.W. Ludwig, *General relationship between the entanglement spectrum and the edge state spectrum of topological quantum states*, *Phys. Rev. Lett.* **108** (2012) 196402.
- [19] F. Pollmann, A.M. Turner, E. Berg and M. Oshikawa, *Entanglement spectrum of a topological phase in one dimension*, *Phys. Rev. B* **81** (2010) 064439.
- [20] H. Yao and X.-L. Qi, *Entanglement entropy and entanglement spectrum of the kitaev model*, *Phys. Rev. Lett.* **105** (2010) 080501.
- [21] Z. Liu, H.-L. Guo, V. Vedral and H. Fan, *Entanglement spectrum: Identification of the transition from vortex-liquid to vortex-lattice state in a weakly interacting rotating bose-einstein condensate*, *Phys. Rev. A* **83** (2011) 013620.
- [22] P. Calabrese and A. Lefevre, *Entanglement spectrum in one-dimensional systems*, *Phys. Rev. A* **78** (2008) 032329.
- [23] A.M. Läuchli, E.J. Bergholtz, J. Suorsa and M. Haque, *Disentangling entanglement spectra of fractional quantum hall states on torus geometries*, *Phys. Rev. Lett.* **104** (2010) 156404.
- [24] J. Schliemann, *Entanglement spectrum and entanglement thermodynamics of quantum hall bilayers at $\nu = 1$* , *Phys. Rev. B* **83** (2011) 115322.

- [25] B.I. Halperin, *Quantized hall conductance, current-carrying edge states, and the existence of extended states in a two-dimensional disordered potential*, *Phys. Rev. B* **25** (1982) 2185.
- [26] X.-L. Qi, H. Katsura and A.W.W. Ludwig, *General relationship between the entanglement spectrum and the edge state spectrum of topological quantum states*, *Phys. Rev. Lett.* **108** (2012) 196402.
- [27] N. Laflorencie, *Quantum entanglement in condensed matter systems*, *Physics Reports* **646** (2016) 1.
- [28] B. Blok and X.G. Wen, *Effective theories of the fractional quantum hall effect: Hierarchy construction*, *Phys. Rev. B* **42** (1990) 8145.
- [29] N. Read, *Excitation structure of the hierarchy scheme in the fractional quantum hall effect*, *Phys. Rev. Lett.* **65** (1990) 1502.
- [30] D.S. Rokhsar and S.A. Kivelson, *Superconductivity and the quantum hard-core dimer gas*, *Phys. Rev. Lett.* **61** (1988) 2376.
- [31] N. Read and B. Chakraborty, *Statistics of the excitations of the resonating-valence-bond state*, *Phys. Rev. B* **40** (1989) 7133.
- [32] R. Moessner and S.L. Sondhi, *Resonating valence bond phase in the triangular lattice quantum dimer model*, *Phys. Rev. Lett.* **86** (2001) 1881.
- [33] E. Ardonne, P. Fendley and E. Fradkin, *Topological order and conformal quantum critical points*, *Annals of Physics* **310** (2004) 493.
- [34] M.A. Levin and X.-G. Wen, *String-net condensation: A physical mechanism for topological phases*, *Phys. Rev. B* **71** (2005) 045110.
- [35] A. Kitaev and J. Preskill, *Topological entanglement entropy*, *Physical review letters* **96** (2006) 110404.
- [36] H.-C. Jiang, Z. Wang and L. Balents, *Identifying topological order by entanglement entropy*, *Nature Physics* **8** (2012) 902.
- [37] A. Hamma, R. Ionicioiu and P. Zanardi, *Bipartite entanglement and entropic boundary law in lattice spin systems*, *Phys. Rev. A* **71** (2005) 022315.
- [38] M. Levin and X.-G. Wen, *Detecting topological order in a ground state wave function*, *Phys. Rev. Lett.* **96** (2006) 110405.
- [39] A. Kitaev and J. Preskill, *Topological entanglement entropy*, *Phys. Rev. Lett.* **96** (2006) 110404.
- [40] Y. Zhang, T. Grover, A. Turner, M. Oshikawa and A. Vishwanath, *Quasiparticle statistics and braiding from ground-state entanglement*, *Phys. Rev. B* **85** (2012) 235151.
- [41] T. Grover, A.M. Turner and A. Vishwanath, *Entanglement entropy of gapped phases and topological order in three dimensions*, *Phys. Rev. B* **84** (2011) 195120.
- [42] A. Hamma and D.A. Lidar, *Adiabatic preparation of topological order*, *Phys. Rev. Lett.* **100** (2008) 030502.
- [43] T. Lan and X.-G. Wen, *Topological quasiparticles and the holographic bulk-edge relation in $(2+1)$ -dimensional string-net models*, *Phys. Rev. B* **90** (2014) 115119.
- [44] P. Fendley, S.V. Isakov and M. Troyer, *Fibonacci topological order from quantum nets*, *Phys. Rev. Lett.* **110** (2013) 260408.
- [45] Z.-C. Gu, M. Levin, B. Swingle and X.-G. Wen, *Tensor-product representations for string-net condensed states*, *Phys. Rev. B* **79** (2009) 085118.
- [46] K. Slagle, D. Aasen and D. Williamson, *Foliated Field Theory and String-Membrane-Net Condensation Picture of Fracton Order*, *SciPost Phys.* **6** (2019) 43.
- [47] S. Das and S. Shankaranarayanan, *How robust is the entanglement entropy-area relation?*, *Phys. Rev. D* **73** (2006) 121701.
- [48] M. Cramer, J. Eisert, M.B. Plenio and J. Dreißig, *Entanglement-area law for general bosonic harmonic lattice systems*, *Phys. Rev. A* **73** (2006) 012309.

- [49] O. Vafek and A. Vishwanath, *Dirac fermions in solids: From high- T_c cuprates and graphene to topological insulators and weyl semimetals*, *Annual Review of Condensed Matter Physics* **5** (2014) 83.
- [50] B.A. Bernevig and T.L. Hughes, *Topological Insulators and Topological Superconductors*, Princeton University Press (2013).
- [51] J. Cayssol, *Introduction to dirac materials and topological insulators*, *Comptes Rendus Physique* **14** (2013) 760.
- [52] R. Moessner and J.E. Moore, *Topological Phases of Matter*, Cambridge University Press (2021), 10.1017/9781316226308.
- [53] S. Rachel, *Interacting topological insulators: a review*, *Reports on Progress in Physics* **81** (2018) 116501.
- [54] J. Wang, S. Deng, Z. Liu and Z. Liu, *The rare two-dimensional materials with Dirac cones*, *National Science Review* **2** (2015) 22.
- [55] M. Wu, Z. Wang, J. Liu, W. Li, H. Fu, L. Sun et al., *Conetronics in 2d metal-organic frameworks: double/half dirac cones and quantum anomalous hall effect*, *2D Materials* **4** (2016) 015015.
- [56] X. Ni, H. Huang and J.-L. Brédas, *Emergence of a two-dimensional topological dirac semimetal phase in a phthalocyanine-based covalent organic framework*, *Chemistry of Materials* **34** (2022) 3178.
- [57] S.-L. Zhu, B. Wang and L.-M. Duan, *Simulation and detection of dirac fermions with cold atoms in an optical lattice*, *Phys. Rev. Lett.* **98** (2007) 260402.
- [58] L. Lepori, G. Mussardo and A. Trombettoni, *(3+1) massive dirac fermions with ultracold atoms in frustrated cubic optical lattices*, *EPL (Europhysics Letters)* **92** (2010) 50003.
- [59] O. Boada, A. Celi, J.I. Latorre and M. Lewenstein, *Dirac equation for cold atoms in artificial curved spacetimes*, *New Journal of Physics* **13** (2011) 035002.
- [60] Y. Kuno, I. Ichinose and Y. Takahashi, *Generalized lattice wilson–dirac fermions in (1 + 1) dimensions for atomic quantum simulation and topological phases*, *Scientific Reports* **8** (2018) 10699.
- [61] K.K. Gomes, W. Mar, W. Ko, F. Guinea and H.C. Manoharan, *Designer dirac fermions and topological phases in molecular graphene*, *Nature* **483** (2012) 306.
- [62] X. Yuan, C. Zhang, Y. Liu, A. Narayan, C. Song, S. Shen et al., *Observation of quasi-two-dimensional dirac fermions in zrte5*, *NPG Asia Materials* **8** (2016) e325.
- [63] M. Bellec, U. Kuhl, G. Montambaux and F. Mortessagne, *Topological transition of dirac points in a microwave experiment*, *Phys. Rev. Lett.* **110** (2013) 033902.
- [64] G. Vidal, J.I. Latorre, E. Rico and A. Kitaev, *Entanglement in quantum critical phenomena*, *Physical review letters* **90** (2003) 227902.
- [65] J.I. Latorre, E. Rico and G. Vidal, *Ground state entanglement in quantum spin chains*, .
- [66] J.I. Latorre, C.A. Lütken, E. Rico and G. Vidal, *Fine-grained entanglement loss along renormalization-group flows*, *Phys. Rev. A* **71** (2005) 034301.
- [67] B.-Q. Jin and V.E. Korepin, *Quantum spin chain, toeplitz determinants and the fisher—hartwig conjecture*, *Journal of Statistical Physics* **116** (2004) 79.
- [68] N. Lambert, C. Emary and T. Brandes, *Entanglement and the phase transition in single-mode superradiance*, *Phys. Rev. Lett.* **92** (2004) 073602.
- [69] C. Holzhey, F. Larsen and F. Wilczek, *Geometric and renormalized entropy in conformal field theory*, *Nuclear Physics B* **424** (1994) 443.
- [70] H. Casini and M. Huerta, *A finite entanglement entropy and the c-theorem*, *Physics Letters B* **600** (2004) 142.
- [71] P. Calabrese and J. Cardy, *Entanglement entropy and quantum field theory*, *Journal of Statistical Mechanics: Theory and Experiment* **2004** (2004) P06002.
- [72] T.J. Osborne and M.A. Nielsen, *Entanglement in a simple quantum phase transition*, *Physical Review A* **66** (2002) 032110.

- [73] A. Osterloh, L. Amico, G. Falci and R. Fazio, *Scaling of entanglement close to a quantum phase transition*, *Nature* **416** (2002) 608.
- [74] H. Casini, C.D. Fosco and M. Huerta, *Entanglement and alpha entropies for a massive dirac field in two dimensions*, *Journal of Statistical Mechanics: Theory and Experiment* **2005** (2005) P07007.
- [75] J.L. Cardy, O.A. Castro-Alvaredo and B. Doyon, *Form factors of branch-point twist fields in quantum integrable models and entanglement entropy*, *Journal of Statistical Physics* **130** (2008) 129.
- [76] H. Casini and M. Huerta, *Reduced density matrix and internal dynamics for multicomponent regions*, *Classical and Quantum Gravity* **26** (2009) 185005.
- [77] B. Doyon, *Bipartite entanglement entropy in massive two-dimensional quantum field theory*, *Phys. Rev. Lett.* **102** (2009) 031602.
- [78] H. Casini and M. Huerta, *Entanglement entropy in free quantum field theory*, *Journal of Physics A: Mathematical and Theoretical* **42** (2009) 504007.
- [79] D. Gioev and I. Klich, *Entanglement entropy of fermions in any dimension and the widom conjecture*, *Physical review letters* **96** (2006) 100503.
- [80] M.M. Wolf, *Violation of the entropic area law for fermions*, *Phys. Rev. Lett.* **96** (2006) 010404.
- [81] W. Li, L. Ding, R. Yu, T. Roscilde and S. Haas, *Scaling behavior of entanglement in two- and three-dimensional free-fermion systems*, *Phys. Rev. B* **74** (2006) 073103.
- [82] T. Barthel, M.-C. Chung and U. Schollwöck, *Entanglement scaling in critical two-dimensional fermionic and bosonic systems*, *Phys. Rev. A* **74** (2006) 022329.
- [83] S. Farkas and Z. Zimborás, *The von neumann entropy asymptotics in multidimensional fermionic systems*, *Journal of Mathematical Physics* **48** (2007) 102110.
- [84] M.M. Wolf, F. Verstraete, M.B. Hastings and J.I. Cirac, *Area laws in quantum systems: mutual information and correlations*, *Physical review letters* **100** (2008) 070502.
- [85] O.A. Castro-Alvaredo and B. Doyon, *Bi-partite entanglement entropy in massive (1+1)-dimensional quantum field theories*, *Journal of Physics A: Mathematical and Theoretical* **42** (2009) 504006.
- [86] B. Swingle, *Entanglement entropy and the fermi surface*, *Physical review letters* **105** (2010) 050502.
- [87] R. Helling, H. Leschke and W. Spitzer, *A Special Case of a Conjecture by Widom with Implications to Fermionic Entanglement Entropy*, *International Mathematics Research Notices* **2011** (2010) 1451.
- [88] P. Calabrese, M. Mintchev and E. Vicari, *Entanglement entropies in free-fermion gases for arbitrary dimension*, *EPL (Europhysics Letters)* **97** (2012) 20009.
- [89] B. Swingle, *Rényi entropy, mutual information, and fluctuation properties of fermi liquids*, *Phys. Rev. B* **86** (2012) 045109.
- [90] P. Calabrese, M. Mintchev and E. Vicari, *Exact relations between particle fluctuations and entanglement in fermi gases*, *EPL (Europhysics Letters)* **98** (2012) 20003.
- [91] M.T. Tan and S. Ryu, *Particle number fluctuations, renyi entropy, and symmetry-resolved entanglement entropy in a two-dimensional fermi gas from multidimensional bosonization*, *Phys. Rev. B* **101** (2020) 235169.
- [92] S. Murciano, P. Ruggiero and P. Calabrese, *Symmetry resolved entanglement in two-dimensional systems via dimensional reduction*, *Journal of Statistical Mechanics: Theory and Experiment* **2020** (2020) 083102.
- [93] X. Chen, W. Witczak-Krempa, T. Faulkner and E. Fradkin, *Two-cylinder entanglement entropy under a twist*, *Journal of Statistical Mechanics: Theory and Experiment* **2017** (2017) 043104.
- [94] P. Bueno and W. Witczak-Krempa, *Holographic torus entanglement and its renormalization group flow*, *Phys. Rev. D* **95** (2017) 066007.
- [95] M.A. Metlitski, C.A. Fuertes and S. Sachdev, *Entanglement entropy in the $o(n)$ model*, *Phys. Rev. B* **80** (2009) 115122.
- [96] R.E. Arias, D.D. Blanco and H. Casini, *Entanglement entropy as a witness of the aharonov–bohm effect in QFT*, *Journal of Physics A: Mathematical and Theoretical* **48** (2015) 145401.

- [97] S. Whitsitt, W. Witczak-Krempa and S. Sachdev, *Entanglement entropy of large- n wilson-fisher conformal field theory*, *Phys. Rev. B* **95** (2017) 045148.
- [98] W. Zhu, X. Chen, Y.-C. He and W. Witczak-Krempa, *Entanglement signatures of emergent dirac fermions: Kagome spin liquid and quantum criticality*, *Science Advances* **4** (2018) eaat5535 [<https://www.science.org/doi/pdf/10.1126/sciadv.aat5535>].
- [99] S. Hu, W. Zhu, S. Eggert and Y.-C. He, *Dirac spin liquid on the spin-1/2 triangular heisenberg antiferromagnet*, *Phys. Rev. Lett.* **123** (2019) 207203.
- [100] V. Crépel, A. Hackenbroich, N. Regnault and B. Estienne, *Universal signatures of dirac fermions in entanglement and charge fluctuations*, *Phys. Rev. B* **103** (2021) 235108.
- [101] J. Luttinger, *Fermi surface and some simple equilibrium properties of a system of interacting fermions*, *Physical Review* **119** (1960) 1153.
- [102] J.M. Luttinger and J.C. Ward, *Ground-state energy of a many-fermion system. ii*, *Physical Review* **118** (1960) 1417.
- [103] M. Oshikawa, *Topological approach to luttinger's theorem and the fermi surface of a kondo lattice*, *Physical Review Letters* **84** (2000) 3370.
- [104] K. Seki and S. Yunoki, *Topological interpretation of the luttinger theorem*, *Physical Review B* **96** (2017) 085124.
- [105] J.T. Heath and K.S. Bedell, *Necessary and sufficient conditions for the validity of luttinger's theorem*, *New Journal of Physics* **22** (2020) 063011.
- [106] A. Mukherjee and S. Lal, *Unitary renormalisation group for correlated electrons-i: a tensor network approach*, *Nuclear Physics B* **960** (2020) 115170.
- [107] A. Mukherjee and S. Lal, *Unitary renormalisation group for correlated electrons-ii: insights on fermionic criticality*, *Nuclear Physics B* **960** (2020) 115163.
- [108] G.t. Hooft, *Dimensional reduction in quantum gravity*, *arXiv:gr-qc/9310026* (1993) .
- [109] E. Verlinde, *On the origin of gravity and the laws of newton*, *Journal of High Energy Physics* **2011** (2011) 29.
- [110] H.-W. Chiang, Y.-C. Hu and P. Chen, *Quantization of spacetime based on a spacetime interval operator*, *Phys. Rev. D* **93** (2016) 084043.
- [111] M. Van Raamsdonk, *Building up spacetime with quantum entanglement*, *General Relativity and Gravitation* **42** (2010) 2323.
- [112] M.V. Raamsdonk, *Lectures on gravity and entanglement*, in *New Frontiers in Fields and Strings*, pp. 297–351 (2017), DOI.
- [113] X.-L. Qi, *Exact holographic mapping and emergent space-time geometry*, *arXiv:1309.6282* (2013) .
- [114] C.H. Lee and X.-L. Qi, *Exact holographic mapping in free fermion systems*, *Physical Review B* **93** (2016) 035112.
- [115] R. Bousso, *The holographic principle*, *Rev. Mod. Phys.* **74** (2002) 825.
- [116] J. Katz and J. Sheng, *Applications of holography in fluid mechanics and particle dynamics*, *Annual Review of Fluid Mechanics* **42** (2010) 531.
- [117] A. Green, *An introduction to gauge-gravity duality and its application in condensed matter*, *Contemporary Physics* **54** (2013) 33.
- [118] J. Zaanen, Y. Liu, Y.-W. Sun and K. Schalm, *Holographic Duality in Condensed Matter Physics*, Cambridge University Press (2015), [10.1017/CBO9781139942492](https://doi.org/10.1017/CBO9781139942492).
- [119] A. Joseph, *Review of lattice supersymmetry and gauge-gravity duality*, *International Journal of Modern Physics A* **30** (2015) 1530054.
- [120] H. Năstase, *Introduction to the AdS/CFT Correspondence*, Cambridge University Press (2015), [10.1017/CBO9781316090954](https://doi.org/10.1017/CBO9781316090954).
- [121] M. Ammon and J. Erdmenger, *Gauge/Gravity Duality*, Cambridge University Press (2015), <https://doi.org/10.1017/CBO9780511846373>.

- [122] S.A. Hartnoll, A. Lucas and S. Sachdev, *Holographic Quantum Matter*, The MIT Press (2018).
- [123] G. 't Hooft, *A planar diagram theory for strong interactions*, *Nuclear Physics B* **72** (1974) 461.
- [124] A. Polyakov, *Thermal properties of gauge fields and quark liberation*, *Physics Letters B* **72** (1978) 477.
- [125] A. Polyakov, *Gauge Fields and Strings (1st ed.)*, Routledge (1987).
- [126] D.J. Gross and W. Taylor, *Two-dimensional qcd is a string theory*, *Nuclear Physics B* **400** (1993) 181.
- [127] E. Akhmedov, *A remark on the ads/cft correspondence and the renormalization group flow*, *Physics Letters B* **442** (1998) 152.
- [128] E. Álvarez and C. Gómez, *Geometric holography, the renormalization group and the c-theorem*, *Nuclear Physics B* **541** (1999) 441.
- [129] D.Z. Freedman, S.S. Gubser, K. Pilch and N.P. Warner, *Renormalization group flows from holography-supersymmetry and a c-theorem*, .
- [130] M. Porrati and A. Starinets, *Rg fixed points in supergravity duals of 4-d field theory and asymptotically ads spaces*, *Physics Letters B* **454** (1999) 77.
- [131] S. Kachru, M. Schulz and E. Silverstein, *Self-tuning flat domain walls in 5d gravity and string theory*, *Phys. Rev. D* **62** (2000) 045021.
- [132] L. Girardello, M. Petrini, M. Porrati and A. Zaffaroni, *The supergravity dual of n=1 super yang-mills theory*, *Nuclear Physics B* **569** (2000) 451.
- [133] J. De Boer, E. Verlinde and H. Verlinde, *On the holographic renormalization group*, *Journal of High Energy Physics* **2000** (2000) 003.
- [134] J. de Boer, *The holographic renormalization group*, *Fortschritte der Physik* **49** (2001) 339.
- [135] C.V. Johnson, K.J. Lovis and D.C. Page, *Probing some N = 1 AdS/CFT RG flows*, *Journal of High Energy Physics* **2001** (2001) 036.
- [136] S. Yamaguchi, *AdS branes corresponding to superconformal defects*, *Journal of High Energy Physics* **2003** (2003) 002.
- [137] J.D. Bekenstein, *Black holes and entropy*, *Phys. Rev. D* **7** (1973) 2333.
- [138] S.W. Hawking, *Black hole explosions?*, *Nature* **248** (1974) 30.
- [139] S.W. Hawking, *Particle creation by black holes*, *Communications in Mathematical Physics* **43** (1975) 199.
- [140] J. Maldacena, *The large-n limit of superconformal field theories and supergravity*, *International journal of theoretical physics* **38** (1999) 1113.
- [141] S. Gubser, I. Klebanov and A. Polyakov, *Gauge theory correlators from non-critical string theory*, *Physics Letters B* **428** (1998) 105.
- [142] E. Witten, *Anti-de sitter space and holography*, *Advances in Theoretical and Mathematical Physics* **2** (1998) 253.
- [143] S. Ryu and T. Takayanagi, *Holographic derivation of entanglement entropy from the anti-de sitter space/conformal field theory correspondence*, *Physical review letters* **96** (2006) 181602.
- [144] S. Ryu and T. Takayanagi, *Aspects of holographic entanglement entropy*, *Journal of High Energy Physics* **2006** (2006) 045.
- [145] S.A. Hartnoll, *Lectures on holographic methods for condensed matter physics*, *Classical and Quantum Gravity* **26** (2009) 224002.
- [146] S. Sachdev, *What can gauge-gravity duality teach us about condensed matter physics?*, *Annual Review of Condensed Matter Physics* **3** (2012) 9.
- [147] P.K. Kovtun, D.T. Son and A.O. Starinets, *Viscosity in strongly interacting quantum field theories from black hole physics*, *Phys. Rev. Lett.* **94** (2005) 111601.

- [148] K. Damle and S. Sachdev, *Nonzero-temperature transport near quantum critical points*, *Phys. Rev. B* **56** (1997) 8714.
- [149] S.A. Hartnoll, P.K. Kovtun, M. Müller and S. Sachdev, *Theory of the nernst effect near quantum phase transitions in condensed matter and in dyonic black holes*, *Phys. Rev. B* **76** (2007) 144502.
- [150] S.-S. Lee, *Non-fermi liquid from a charged black hole: A critical fermi ball*, *Phys. Rev. D* **79** (2009) 086006.
- [151] H. Liu, J. McGreevy and D. Vegh, *Non-fermi liquids from holography*, *Phys. Rev. D* **83** (2011) 065029.
- [152] T. Faulkner, H. Liu, J. McGreevy and D. Vegh, *Emergent quantum criticality, fermi surfaces, and ads₂*, *Phys. Rev. D* **83** (2011) 125002.
- [153] M. Čubrović, J. Zaanen and K. Schalm, *String theory, quantum phase transitions, and the emergent fermi liquid*, *Science* **325** (2009) 439
[<https://www.science.org/doi/pdf/10.1126/science.1174962>].
- [154] S.S. Gubser, S.S. Pufu and F.D. Rocha, *Quantum critical superconductors in string theory and m-theory*, *Physics Letters B* **683** (2010) 201.
- [155] J.P. Gauntlett, J. Sonner and T. Wiseman, *Holographic superconductivity in m theory*, *Phys. Rev. Lett.* **103** (2009) 151601.
- [156] S.A. Hartnoll, C.P. Herzog and G.T. Horowitz, *Building a holographic superconductor*, *Phys. Rev. Lett.* **101** (2008) 031601.
- [157] S.A. Hartnoll, C.P. Herzog and G.T. Horowitz, *Holographic superconductors*, *Journal of High Energy Physics* **2008** (2008) 015.
- [158] R. Cai, L. Li, L. Li and R. Yang, *Introduction to holographic superconductor models*, *Science China Physics, Mechanics & Astronomy* **58** (2015) 1.
- [159] C. Wang, D. Zhang, G. Fu and J.-P. Wu, *Analytical study of the holographic superconductor from higher derivative theory*, *Advances in High Energy Physics* **2020** (2020) 5902473.
- [160] A. Donos and J.P. Gauntlett, *Holographic striped phases*, *Journal of High Energy Physics* **2011** (2011) 140.
- [161] A. Donos, *Striped phases from holography*, *Journal of High Energy Physics* **2013** (2013) 59.
- [162] S. Cremonini, L. Li and J. Ren, *Holographic fermions in striped phases*, *Journal of High Energy Physics* **2018** (2018) 80.
- [163] S. Kachru, X. Liu and M. Mulligan, *Gravity duals of lifshitz-like fixed points*, *Phys. Rev. D* **78** (2008) 106005.
- [164] M. Čubrović, Y. Liu, K. Schalm, Y.-W. Sun and J. Zaanen, *Spectral probes of the holographic fermi ground state: Dialing between the electron star and ads dirac hair*, *Phys. Rev. D* **84** (2011) 086002.
- [165] T. Senthil, S. Sachdev and M. Vojta, *Fractionalized fermi liquids*, *Phys. Rev. Lett.* **90** (2003) 216403.
- [166] S. Sachdev, *Model of a fermi liquid using gauge-gravity duality*, *Phys. Rev. D* **84** (2011) 066009.
- [167] S.A. Hartnoll, D.M. Hofman and D. Vegh, *Stellar spectroscopy: Fermions and holographic Lifshitz criticality*, *JHEP* **08** (2011) 096 [[1105.3197](https://arxiv.org/abs/1105.3197)].
- [168] L. Huijse and S. Sachdev, *Fermi surfaces and gauge-gravity duality*, *Phys. Rev. D* **84** (2011) 026001.
- [169] F. Aprile, D. Roest and J.G. Russo, *Holographic superconductors from gauged supergravity*, *Journal of High Energy Physics* **2011** (2011) 40.
- [170] A. Donos and J.P. Gauntlett, *Superfluid black branes in ads₄ × s₇*, *Journal of High Energy Physics* **2011** (2011) 53.
- [171] H. Matsueda, *Multiscale entanglement renormalization ansatz for kondo problem*, *arXiv:1208.2872* (2012) .
- [172] H. Matsueda, M. Ishihara and Y. Hashizume, *Tensor network and a black hole*, *Phys. Rev. D* **87** (2013) 066002.

- [173] H. Matsueda, *Emergent general relativity from fisher information metric*, [arXiv:1310.1831](#) (2013) .
- [174] H. Matsueda, *Geometry and dynamics of emergent spacetime from entanglement spectrum*, .
- [175] B. Czech, *Einstein equations from varying complexity*, *Phys. Rev. Lett.* **120** (2018) 031601.
- [176] T. Faulkner, F.M. Haehl, E. Hijano, O. Parrikar, C. Rabideau and M. Van Raamsdonk, *Nonlinear gravity from entanglement in conformal field theories*, *Journal of High Energy Physics* **2017** (2017) 57.
- [177] T. Faulkner, M. Guica, T. Hartman, R.C. Myers and M. Van Raamsdonk, *Gravitation from entanglement in holographic cfts*, *Journal of High Energy Physics* **2014** (2014) 51.
- [178] Y. Gu, C.H. Lee, X. Wen, G.Y. Cho, S. Ryu and X.-L. Qi, *Holographic duality between $(2 + 1)$ -dimensional quantum anomalous hall state and $(3 + 1)$ -dimensional topological insulators*, *Phys. Rev. B* **94** (2016) 125107.
- [179] X. Wen, G.Y. Cho, P.L.S. Lopes, Y. Gu, X.-L. Qi and S. Ryu, *Holographic entanglement renormalization of topological insulators*, *Phys. Rev. B* **94** (2016) 075124.
- [180] R.G. Leigh, O. Parrikar and A.B. Weiss, *Exact renormalization group and higher-spin holography*, *Phys. Rev. D* **91** (2015) 026002.
- [181] R.G. Leigh, O. Parrikar and A.B. Weiss, *Holographic geometry of the renormalization group and higher spin symmetries*, *Phys. Rev. D* **89** (2014) 106012.
- [182] M.R. Douglas, L. Mazzucato and S.S. Razamat, *Holographic dual of free field theory*, *Phys. Rev. D* **83** (2011) 071701.
- [183] R. de Mello Koch, A. Jevicki, K. Jin and J.a.P. Rodrigues, *ads₄/cft₃ construction from collective fields*, *Phys. Rev. D* **83** (2011) 025006.
- [184] S.-S. Lee, *Holographic description of quantum field theory*, *Nuclear Physics B* **832** (2010) 567.
- [185] S.-S. Lee, *Tasi lectures on emergence of supersymmetry, gauge theory and string in condensed matter systems*, [arXiv:1009.5127](#) (2010) .
- [186] S.-S. Lee, *Background independent holographic description: from matrix field theory to quantum gravity*, *Journal of High Energy Physics* **2012** (2012) 160.
- [187] S.-S. Lee, *Quantum renormalization group and holography*, *Journal of High Energy Physics* **2014** (2014) 76.
- [188] G. Vidal, *Entanglement renormalization*, *Physical review letters* **99** (2007) 220405.
- [189] G. Vidal, *Class of quantum many-body states that can be efficiently simulated*, *Physical review letters* **101** (2008) 110501.
- [190] B. Swingle, *Entanglement renormalization and holography*, *Physical Review D* **86** (2012) 065007.
- [191] G. Evenbly and G. Vidal, *Scaling of entanglement entropy in the (branching) multiscale entanglement renormalization ansatz*, *Phys. Rev. B* **89** (2014) 235113.
- [192] A. Milsted and G. Vidal, *Geometric interpretation of the multi-scale entanglement renormalization ansatz*, .
- [193] G. Evenbly and G. Vidal, *Tensor network states and geometry*, *Journal of Statistical Physics* **145** (2011) 891.
- [194] J. Reyes and M. Stoudenmire, *A multi-scale tensor network architecture for classification and regression*, [arXiv:2001.08286](#) (2020) .
- [195] N.A. McMahon, S. Singh and G.K. Brennen, *A holographic duality from lifted tensor networks*, *npj Quantum Information* **6** (2020) 36.
- [196] A. Mukherjee and S. Lal, *Superconductivity from repulsion in the doped 2d electronic hubbard model: an entanglement perspective*, *Journal of Physics: Condensed Matter* **34** (2022) 275601.
- [197] K.-S. Kim, S.B. Chung, C. Park and J.-H. Han, *Emergent holographic description for the kondo effect: Comparison with bethe ansatz*, *Phys. Rev. D* **99** (2019) 105012.

- [198] K.-S. Kim, M. Park, J. Cho and C. Park, *Emergent geometric description for a topological phase transition in the kitaev superconductor model*, *Phys. Rev. D* **96** (2017) 086015.
- [199] K.-S. Kim and C. Park, *Emergent geometry from field theory: Wilson's renormalization group revisited*, *Phys. Rev. D* **93** (2016) 121702.
- [200] K.-S. Kim, *Emergent dual holographic description for interacting dirac fermions in the large n limit*, *Phys. Rev. D* **102** (2020) 086014.
- [201] K.-S. Kim, *Geometric encoding of renormalization group β -functions in an emergent holographic dual description*, *Phys. Rev. D* **102** (2020) 026022.
- [202] K.-S. Kim, *Emergent geometry in recursive renormalization group transformations*, *Nuclear Physics B* **959** (2020) 115144.
- [203] K.-S. Kim, *Emergent dual holographic description for interacting dirac fermions in the large n limit*, *Phys. Rev. D* **102** (2020) 086014.
- [204] K.-S. Kim and S. Ryu, *Entanglement transfer from quantum matter to classical geometry in an emergent holographic dual description of a scalar field theory*, *Journal of High Energy Physics* **2021** (2021) 260.
- [205] K.G. Wilson, *The renormalization group: Critical phenomena and the kondo problem*, *Rev. Mod. Phys.* **47** (1975) 773.
- [206] H.R. Krishna-murthy, J.W. Wilkins and K.G. Wilson, *Renormalization-group approach to the anderson model of dilute magnetic alloys. i. static properties for the symmetric case*, *Phys. Rev. B* **21** (1980) 1003.
- [207] S. Patra, S. Basu and S. Lal, *Unveiling topological order through multipartite entanglement*, *Phys. Rev. A* **105** (2022) 052428.
- [208] M.-C. Chung and I. Peschel, *Density-matrix spectra for two-dimensional quantum systems*, *Phys. Rev. B* **62** (2000) 4191.
- [209] H.-Z. Lu, W.-Y. Shan, W. Yao, Q. Niu and S.-Q. Shen, *Massive dirac fermions and spin physics in an ultrathin film of topological insulator*, *Phys. Rev. B* **81** (2010) 115407.
- [210] W. Zhao, C.X. Trang, Q. Li, L. Chen, Z. Yue, A. Bake et al., *Massive dirac fermions and strong shubnikov-de haas oscillations in single crystals of the topological insulator Bi_2Se_3 doped with sm and fe*, *Phys. Rev. B* **104** (2021) 085153.
- [211] B. Hunt, J.D. Sanchez-Yamagishi, A.F. Young, M. Yankowitz, B.J. LeRoy, K. Watanabe et al., *Massive dirac fermions and hofstadter butterfly in a van der waals heterostructure*, *Science* **340** (2013) 1427.
- [212] A. Abanov and P. Wiegmann, *Theta-terms in nonlinear sigma-models*, *Nuclear Physics B* **570** (2000) 685.
- [213] S. Pal, A. Mukherjee and S. Lal, *Correlated spin liquids in the quantum kagome antiferromagnet at finite field: a renormalization group analysis*, *New Journal of Physics* **21** (2019) 023019.
- [214] M. Blasone, F. Dell'Anno, S. De Siena and F. Illuminati, *Hierarchies of geometric entanglement*, *Phys. Rev. A* **77** (2008) 062304.
- [215] K. Hyatt, J.R. Garrison and B. Bauer, *Extracting entanglement geometry from quantum states*, *Physical review letters* **119** (2017) 140502.
- [216] A. Mukherjee and S. Lal, *Superconductivity from repulsion in the doped 2d electronic hubbard model: an entanglement perspective*, *Journal of Physics: Condensed Matter* **34** (2022) 275601.
- [217] R.C. Myers and A. Sinha, *Seeing a c-theorem with holography*, *Phys. Rev. D* **82** (2010) 046006.
- [218] R.C. Myers and A. Sinha, *Holographic c-theorems in arbitrary dimensions*, *Journal of High Energy Physics* **2011** (2011) 125.
- [219] C.-S. Chu and D. Giataganas, *c-theorem for anisotropic rg flows from holographic entanglement entropy*, *Phys. Rev. D* **101** (2020) 046007.

- [220] C. Cao, S.M. Carroll and S. Michalakis, *Space from hilbert space: Recovering geometry from bulk entanglement*, *Phys. Rev. D* **95** (2017) 024031.
- [221] S. Singha Roy, S.N. Santalla, J. Rodríguez-Laguna and G. Sierra, *Entanglement as geometry and flow*, *Phys. Rev. B* **101** (2020) 195134.
- [222] S. Bau and A.F. Beardon, *The metric dimension of metric spaces*, *Computational Methods and Function Theory* **13** (2013) 295.
- [223] S. Kar, *Geometry of renormalization group flows in theory space*, *Phys. Rev. D* **64** (2001) 105017.
- [224] S. Kar and S. Sengupta, *The raychaudhuri equations: A brief review*, *Pramana* **69** (2007) 49.
- [225] I. Peschel, *Calculation of reduced density matrices from correlation functions*, *Journal of Physics A: Mathematical and General* **36** (2003) L205.
- [226] A. Alexandradinata, T.L. Hughes and B.A. Bernevig, *Trace index and spectral flow in the entanglement spectrum of topological insulators*, *Phys. Rev. B* **84** (2011) 195103.
- [227] D. Thouless, M. Kohmoto, M. Nightingale and M. Den Nijs, *Quantized hall conductance in a two-dimensional periodic potential*, *Physical Review Letters* **49** (1982) 405.
- [228] M.O. Flynn, L.-H. Tang, A. Chandran and C.R. Laumann, *Momentum space entanglement of interacting fermions*, 2022. 10.48550/ARXIV.2203.08154.
- [229] V. Balasubramanian, M.B. McDermott and M. Van Raamsdonk, *Momentum-space entanglement and renormalization in quantum field theory*, *Physical Review D* **86** (2012) 045014.
- [230] T. Hsu, M. McDermott and M. Van Raamsdonk, *Momentum-space entanglement for interacting fermions at finite density.*, *J. High Energy. Phys.* **121** (2013) (2013) .
- [231] M.H. Martins Costa, J. van den Brink, F.S. Nogueira and G.a.I. Krein, *Momentum space entanglement from the wilsonian effective action*, *Phys. Rev. D* **106** (2022) 065024.
- [232] S. Patra, A. Mukherjee and S. Lal, *Universal entanglement signatures of quantum liquids as a guide to fermionic criticality*, 2022. 10.48550/ARXIV.2205.11123.
- [233] V. Balasubramanian and P. Kraus, *Spacetime and the holographic renormalization group*, *Physical Review Letters* **83** (1999) 3605.
- [234] V. Balasubramanian, A. Bernamonti, N. Copland, B. Craps and F. Galli, *Thermalization of mutual and tripartite information in strongly coupled two dimensional conformal field theories*, *Phys. Rev. D* **84** (2011) 105017.
- [235] M. Asadi and M. Ali-Akbari, *Holographic mutual and tripartite information in a symmetry breaking quench*, *Physics Letters B* **785** (2018) 409.
- [236] M. Ali-Akbari, M. Asadi and M. Rahimi, *Holographic mutual and tripartite information in a non-conformal background*, *arXiv:1907.08917* (2019) .

A Appendix: Reduction of the 2 + 1–D system to a tower of 1 + 1–D massive modes

In the absence of the gauge field, the Lagrangian for 2 + 1–dimensional massive non-interacting relativistic electrons (in natural units) is

$$\mathcal{L} = \int dx dy \bar{\psi}(x, y) [i\gamma^\mu \partial_\mu - m] \psi(x, y) . \quad (\text{A.1})$$

The integral ranges over the area of the torus on which the electrons reside, and the time dependence of the fields has been suppressed. Each component $\psi^a, a = 0, 1, 2, 3$, of the Dirac spinor $\psi = (\psi^0 \ \psi^1 \ \psi^2 \ \psi^3)$ satisfies the Dirac equation

$$[i\gamma^\mu \partial_\mu - m] \psi^a(x, y) = 0 , \quad (\text{A.2})$$

which is equivalent to the form

$$\int dx \bar{\psi}^a(x, y) [i\partial^\nu \gamma_\nu + m] [i\gamma^\mu \partial_\mu - m] \psi^a(x, y) = 0. \quad (\text{A.3})$$

Due to the periodic boundary conditions (PBCs) in the x -direction, the momenta k_x are quantised: $k_x^n = \frac{2\pi n}{L_x}, n \in \mathbb{Z}$. We expand the fields $\psi^a(x, y)$ in these momenta:

$$\psi^a(x, y) = \sum_{n=-\infty}^{\infty} e^{ik_x^n x} \psi^a(k_x^n, y). \quad (\text{A.4})$$

Writing the Dirac equation in terms of the dual fields $\psi^a(k_x^n, y)$ gives

$$\sum_{m,n} \left(\bar{\psi}^a(k_x^m, y) e^{-ik_x^m x} \right) [i\partial^\nu \gamma_\nu + m] [i\gamma^\mu \partial_\mu - m] \left(e^{ik_x^n x} \psi^a(k_x^n, y) \right) = 0, \quad (\text{A.5})$$

where

$$[i\gamma^\mu \partial_\mu - m] \left(e^{ik_x^n x} \psi^a \right) = e^{ik_x^n x} [i\gamma^\mu \partial_\mu - (\gamma^x k_x^n + m)] \psi^a. \quad (\text{A.6})$$

Similarly,

$$\left(\bar{\psi}^a(k_x^m, y) e^{-ik_x^m x} \right) [i\partial^\nu \gamma_\nu + m] = \left[[i\gamma^\nu \partial_\nu + m] \left(e^{ik_x^m x} \gamma_0 \psi^a \right) \right]^\dagger = \bar{\psi}^a e^{-ik_x^m x} [i\partial^\nu \gamma_\nu - (\gamma^x k_x^m - m)]. \quad (\text{A.7})$$

Substituting these into the equation eq.(A.5) gives

$$\sum_n \int dy \bar{\psi}^a(k_x^n, y) \left[\partial_\mu \partial^\mu + k_x^{n2} + m^2 \right] \psi^a(k_x^n, y) = 0, \quad (\text{A.8})$$

where we have used $\int dx e^{ix(k_x^m - k_x^n)} = \delta_{m,n}$.

B Appendix: Evaluation of the multi-partite information

We define the multipartite information among g sets $\{\mathcal{A}_{i,z}\}$ as [207]

$$I_{\{\mathcal{A}_{i,z}\}}^g = \sum_{r=1}^g (-1)^{r-1} \sum_{\beta \in \mathcal{P}(\{\mathcal{A}_{i,z}\})}^{|\beta|=r} S_\beta, \quad (\text{B.1})$$

where $\mathcal{P}(\{\mathcal{A}_{i,z}\})$ is the power set of $\{\mathcal{A}_{i,z}\}$, and $|\beta| = r$ implies that we sum only over those sets β that have r number of elements in them. We will first evaluate the internal sum σ_r over the set β for a general r :

$$\sigma_r = \sum_{\beta \in \mathcal{P}(\{\mathcal{A}_{i,z}\})}^{|\beta|=r} S_\beta. \quad (\text{B.2})$$

For this, we first note that following eq. (3.15), the entanglement entropy (EE) of the union of a given sequence of sets $\{i\}$ is given by the EE of the set with the highest (lowest) index for a positive (negative) z . As a result, the EE S_β for the set β is simply $S_\beta = \theta(z) S_{\min(\beta)} + \theta(-z) S_{\max(\beta)}$. If $n_j^{(r,+)}$ ($n_j^{(r,-)}$) is the number of sets of cardinality r that have the element $\mathcal{A}_{j,z}$ as the element with the smallest (largest) index j , the internal sum can be written as

$$\sigma_r = \sum_{j=1}^{g-(r-1)} \theta(z) n_j^{(r,+)} S_{j,z} + \sum_{j=r}^g \theta(-z) n_j^{(r,-)} S_{j,z}. \quad (\text{B.3})$$

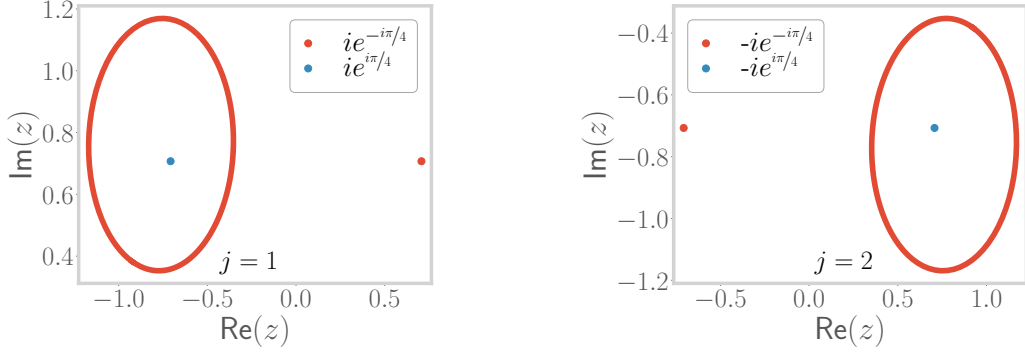


Figure 16. Contours $z(\mathcal{C}_j)$ for two values of j employed for evaluating the integral eq.(C.1), and the locations of the poles z_{\pm}^{\pm} . For each j , only one pole (shown in blue) contributes, as the other (shown in red) is not enclosed by the contour.

The number $n_j^{(r,+)}$ corresponds to the number of ways one can pick $r-1$ elements out of a set of $g-j$ elements: $n_j^{(r,+)} = \binom{g-j}{r-1}$. Similarly, $n_j^{(r,-)}$ corresponds to the number of ways one can pick $r-1$ elements out of a set of j elements: $n_j^{(r,-)} = \binom{j}{r-1}$. We can also extend the limits on the two summations by defining $\binom{n}{m} = 0$ for $n < m$. With these considerations, eq. (B.3) takes the form

$$\sigma_r = \sum_{j=1}^g \left[\theta(z) \binom{g-j}{r-1} + \theta(-z) \binom{j}{r-1} \right] S_{j,z}. \quad (\text{B.4})$$

This can now be substituted into the full expression for the multipartite equation, giving

$$\begin{aligned} I_{\{\mathcal{A}_{i,z}\}}^g &= \sum_{r=1}^g (-1)^{r-1} \sum_{j=1}^g \left[\theta(z) \binom{g-j}{r-1} + \theta(-z) \binom{j}{r-1} \right] S_{j,z} \\ &= \sum_{j=1}^g S_{j,z} \left[\theta(z) \sum_{r=0}^{g-j} (-1)^r \binom{g-j}{r} + \theta(-z) \sum_{r=0}^j (-1)^r \binom{j}{r} \right]. \end{aligned} \quad (\text{B.5})$$

From the binomial theorem, we can now recognise each internal sum as over r as a polynomial expansion. That is, upon comparing with $(x-1)^n = \sum_{m=0}^n \binom{n}{m} (-1)^m x^{n-m}$, we obtain $\sum_{r=0}^{g-j} (-1)^r \binom{g-j}{r} = \lim_{x \rightarrow 1} (x-1)^{g-j} = \delta_{g,j}$. Similarly, the other sum evaluates to $\delta_{j,0}$. Substituting these into the expression for $I_{\{\mathcal{A}_{i,z}\}}^g$ gives

$$I_{\{\mathcal{A}_{i,z}\}}^g = \sum_{j=1}^g S_{j,z} [\theta(z)\delta_{g,j} + \theta(-z)\delta_{j,0}] = \theta(z)S_g + \theta(-z)S_0. \quad (\text{B.6})$$

By noting that S_g and S_0 are, respectively, the EE of the intersection set of $\{\mathcal{S}_{i,z}\}$, one can combine the two terms in the previous equation into

$$I_{\{\mathcal{A}_{i,z}\}}^g = \theta(z)S_g + \theta(-z)S_0 = S_{\cap\{\mathcal{A}_{i,z}\}}. \quad (\text{B.7})$$

C Appendix: Evaluation of the contour integral that counts poles

We prove eq. (5.3) in this appendix. The integral in question is given by

$$\mathcal{I} = \oint_{\mathcal{C}_j} \frac{d\phi}{Q_0(\phi)} = \oint_{\mathcal{C}_j} \frac{d\phi}{\frac{1}{\sqrt{2}} - |\sin \pi\phi|}, \quad (\text{C.1})$$

where \mathcal{C}_j is the contour shown in Fig. 12 and the variable ϕ is given by $\phi = \{\phi_j + \frac{1}{8}e^{i\theta} : \theta \in [0, 2\pi]\}$, where $\phi_j = j - \frac{1}{4}$ is the center of the contour. In order to evaluate the integral, we make a variable change: $z = e^{i\pi\phi}$, giving $dz = i\pi z d\phi$ and $\sin \pi\phi = \frac{1}{2i} (z - \frac{1}{z})$. Depending on the value of j , $\sin \pi\phi$ can be either positive or negative. We denote either case by a subscript \mathcal{I}_{\pm} corresponding to the contour \mathcal{C}_{\pm} , giving $|\sin(\pi\phi)| = \pm \sin(\pi\phi)$. Casting the integral in terms of z , we obtain

$$\mathcal{I}_{\pm} = \frac{1}{i\pi} \oint_{z(\mathcal{C}_{\pm})} \frac{dz/z}{\frac{1}{\sqrt{2}} \mp \frac{1}{2i} (z - \frac{1}{z})} = \oint_{z(\mathcal{C}_{\pm})} \frac{\mp \frac{2}{\pi} dz}{\left(z \mp \frac{i}{\sqrt{2}}\right)^2 - \frac{1}{2}}. \quad (\text{C.2})$$

The integrand in \mathcal{I}_+ has two simple poles at $z_{\pm}^{\pm} = \pm i e^{\mp i\pi/4}$. Similarly, the integrand in \mathcal{I}_- has two simple poles at $z_{\pm}^{\pm} = -z_{\pm}^{\pm}$. We plot the contour and the two poles for two contours of opposite signature in Fig. 16; it is clear that only the pole at z_{\pm}^{\pm} contributes to the integral. Using the residue theorem, the integral evaluates to

$$\mathcal{I}_{\pm} = \oint_{z(\mathcal{C}_{\pm})} \frac{\mp \frac{2}{\pi} dz}{(z - z_{\pm}^+)(z - z_{\pm}^-)} = \mp \frac{2}{\pi} 2\pi i \lim_{z \rightarrow z_{\pm}^+} \frac{1}{z - z_{\pm}^-} = \mp 2\sqrt{2}i. \quad (\text{C.3})$$

This proves eq. (5.3).